MASTER THESIS

TITLE: Evaluating LoRa/LoRaWAN performance and scalability

MASTER DEGREE: Master's degree in Applied Telecommunications and Engineering Management (MASTEAM)

AUTHOR: Kazim Iqbal Wani

ADVISOR: Dr. Pere Tuset-Peiró

Tutor: Dr. Carles Gómez Montenegro

DATE: June 11th, 2021

Title: Evaluating LoRa/LoRaWAN performance and scalability

Author: Kazim Iqbal Wani

Advisor: Dr. Pere Tuset-Peiró

Tutor: Dr. Carles Gómez Montenegro

Date: June 11th, 2021

Abstract

The rise and growth of Internet of Things (IoT) – a network connecting physical objects, has made it of paramount importance to have a standard that is capable of providing the required support to this paradigm. Various standards are competing against each other to be the leader in providing the connectivity to the massive network of these objects that are expected to be able to communicate with each other.

Among these standards Low Power Wide Area Networks (LPWANs) are rapidly gaining momentum as a fundamental IoT technology mainly due to their low-power consumption, long range coverage to devices and use of license-free frequency bands. One such standard, LoRa is the focus of this thesis.

One of the main challenges of LoRa/LoRaWAN networks is the maximum number of end devices and the amount of traffic a network can handle. We study and analyse the capacity of a LoRa/LoRaWAN network with an important performance metric, throughput. First, we run simulations to validate the LoRa module in ns-3. Then, we consider a theoretical model which maximizes the capacity of the network and provides ideal number of end devices. We then analyse the theoretical scenario and evaluate the performance of the network by examining the capacity as we vary the path loss. We simulate the network using ns-3 under two different conditions, with and without shadowing, with the real world settings and compare the results with the theoretical scenario.

The results from both the simulations and the theoretical model show that the theoretical model underachieves and does not match the capacity provided completely. The throughput achieved in the simulations is considerably better due to the capture effect property of LoRa/LoRaWAN. This work is important in order to know the limitations of the network before deploying it in the real world.

Contents

INTRODUCTION

The Internet of Things (IoT) [23] [24] is a network consisting of physical devices, a network of interconnected “things”, where the focus is on getting these devices to communicate with each other and send data over Internet with minimal need of human involvement. The devices in the IoT network can be anything from ordinary objects in a house to a complex industrial unit. IoT can be described as a way of connecting real things in the world to the internet.

Billions of devices around the globe are now connected to the Internet, sharing, collecting and storing data. These devices form an essential part of the IoT family. The applications of IoT are widespread, ranging from smart homes, health care and transportation to smart grid, manufacturing and agriculture.

The basic IoT architecture can be separated in three stages: perception, network and application layers as shown in Figure 0.1:

1. In the perception layer the data is collected from IoT devices i.e. sensors and actuators.
2. In the network layer the data collected from the devices is processed and transmitted.
3. In the application layer the data received is made use of and necessary services are provided.

The key factors that have made IoT possible can be summarized as:

- **Availability of low-cost technology:** The availability of affordable sensors and micro-controllers has made IoT viable for more manufactures – small and large scale.

- **Connectivity:** The wide-range of available wireless technologies enable low power communication between the “things” and the sensors to cloud connection for the efficient data transfer.

- **Cloud Computing:** The large strides made in making cloud computing accessible has been significant in the rise of IoT. The reason being that it provides low-cost storing and processing option without the need to actually having to manage it all.

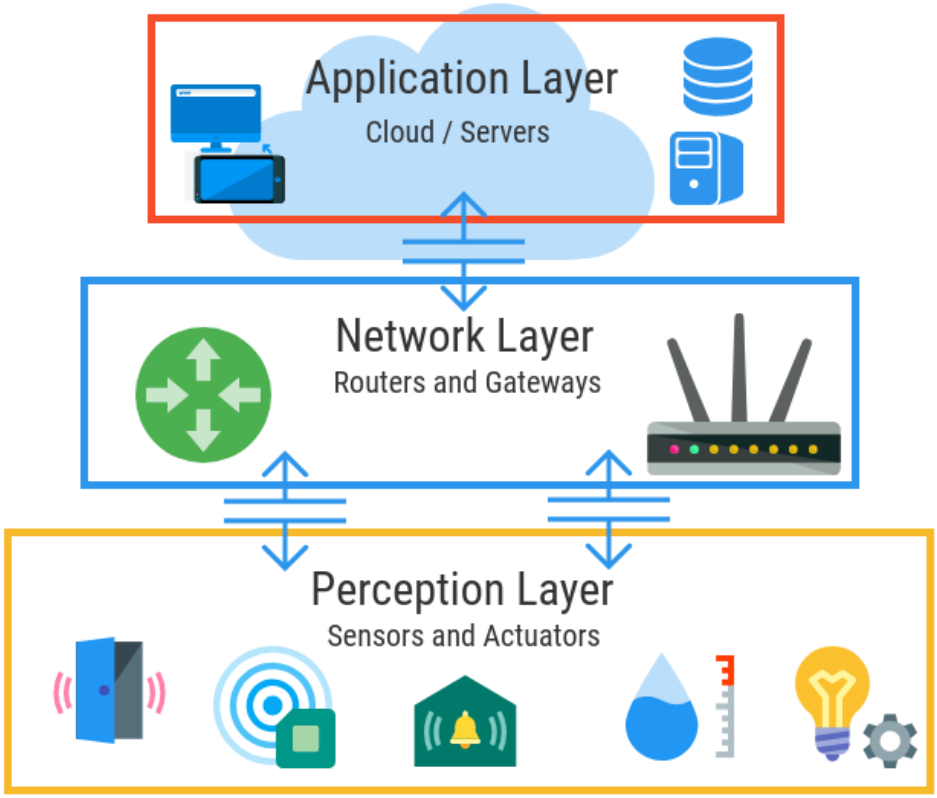

Figure 1.0: IoT structure

- **Advancements in data analytics:** The data analytical capacity has improved significantly in recent times and with the cloud providing a large amount data, it continues to push the boundaries of IoT.

Despite making big strides, IoT scenario does pose some challenges that need to be solved:

- **Battery life:** Majority of the IoT devices collecting and transmitting the data will run on batteries, so it becomes of paramount importance for these devices to have long battery life in order to keep the maintenance cost down.

- **Coverage:** The devices are expected to be able to transmit and receive data under all conditions. It becomes even more important when a service requires time-critical communication needs.

- **Scalability:** With IoT growing at a fast pace and huge number of devices added requiring simultaneous connectivity, IoT network needs to adapt and support the need to have a densely populated wireless environment.

- **Interoperability:** The IoT network is a mix of heterogeneous components and technologies. This makes interoperability vital for IoT to avoid such a situation where connectivity becomes an issue, so an interoperable architecture is a necessity.

There are numerous network standards vying for the spot to be the solution to all the problems posed by the deployment of massive IoT networks. One such solution is – Low Power Wide Area Networks (LPWANs), a technology that proposes wide area connectivity along with the solution to other problems faced by the current IoT paradigm. A LPWAN standard, LoRaWAN is the main focus of this work. We analyse the scope of LoRaWAN and if it could satisfy the capacity requirements needed for the massive IoT deployment. We focus and try to address the problem – Actual Capacity of the LoRaWAN networks.

The goal of this work is to evaluate the performance and scalability of LoRaWAN networks that contain thousands of end devices transmitting concurrently and distributed uniformly around a gateway. This work focuses on achieving the results for actual capacity of a LoRaWAN network rather than a specified one. We use ns-3 to perform the simulations and we study different scenarios, wherein we distribute the end devices differently to investigate the performance of the network regarding the capacity, specifically the results for actual throughput obtained.

In the study of these scenarios the assignment of spreading factors is done based on area and distance from the gateway. We create a simulation environment to evaluate the real performance of LoRaWAN with high number of end devices and with end devices transmitting concurrently with varying spreading factors assigned to them. This study is important, given the fact that a large number of end devices have to be supported by LoRaWAN in a geographical area, where they will be sharing the medium. In order to gauge if all end devices can be supported while also maintaining the quality of service (QoS), we need to understand the limitations regarding the capacity provided by the LoRaWAN networks.

The remainder of the thesis is structured as follows. In chapter 1, we have the description of different IoT technologies that are currently available and offering the solution. In chapter 2, we focus on in-depth description of PHY and MAC layers of LoRa technology. Chapter 3 discusses state of art, past work, our approach and experimental setup and in chapter 4, we discuss the results obtained. In chapter 5, we draw the conclusion of our work and list the possible future works.

Chapter 1: Overview of IoT Technologies

In this chapter we take a look at different solutions proposed for the IoT paradigm and what they offer and how they differ from each other.

1.1. Overview

The rapid success of IoT has given rise to solutions like that of Low Rate Wireless Personal Area Networks (LR-WPANs), Cellular IoT and Low Power Wide Area Network (LPWAN). Low-Power Wide Area Networks (LPWANs) are wireless technologies with characteristics such as large coverage areas, low bandwidth, possibly very small packet and application-layer data sizes, and long battery life operation [1]. The feature of LPWANs is that they send and receive data at infrequent intervals and that results in longer battery life. The data is sent at low data rate, prioritising range over speed. Thus the main characteristics can be summarised as long geographical range, infrequent small amounts of data and low power consumption, for the battery to last for years instead of weeks or months.

Contrary to short range wireless networks (LR-WPAN), that use mesh topology to extend the coverage of the network-Figure 1.1(a), LPWAN is characterised by star topology-Figure 1.1(b). Even though the mesh topology provides robustness, the multi-hop communication causes delay often compensated by high data rates. The topology of LPWAN allows the end devices to have a direct link to the central unit.

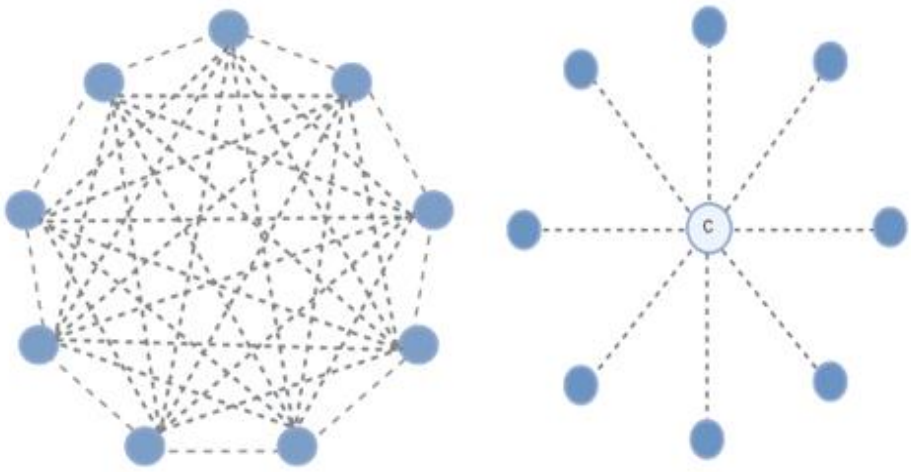

Figure 1.1: Mesh topology and Star topology, c is the central unit

Cellular IoT makes use of the licensed spectrum compared to the other two that operate in the unlicensed spectrum. The shortcomings, range limit and scalability of traditional short range wireless networks are overcome by the LPWAN which offers long range, low power consumption and the capability to connect massive number of devices. There are various types of IoT technologies that provide the solution to the problems associated with the short range wireless networks, with some of them mentioned below. The difference between them is the data rate used, range, the frequency they operate on and the power consumption.

1.2. Low Rate Wireless Personal Area Networks (LR-WPANs)

Low Rate Wireless Personal Network (LR-WPAN) offer wireless connectivity for devices to convey information over short distances. They are typically small networks operating in a small space like a house. They offer low data rates and low power consumption, thus focusing on efficient use of battery.

1.2.1. Zigbee

Zigbee is based on IEEE 802.15.4 standard [25] and offers connectivity up to 100 meters. It provides the data rate between 20 to 250 Kbits/s. It operates in frequencies 868 MHz, 915 MHz and 2.4 GHz, which are available in Europe, North America and worldwide respectively [26]. It provides a range up to 300 meters with Line of Sight (LOS) and up to 100 meters indoors. It supports multiple network topologies such as mesh, star and cluster tree topology, as can be seen in Figure 1.2. The mesh topology is mostly used which increases the reliability of the network and provides redundancy but in turn keeps the nodes awake as they are used as relays, which has a negative impact on their battery life.

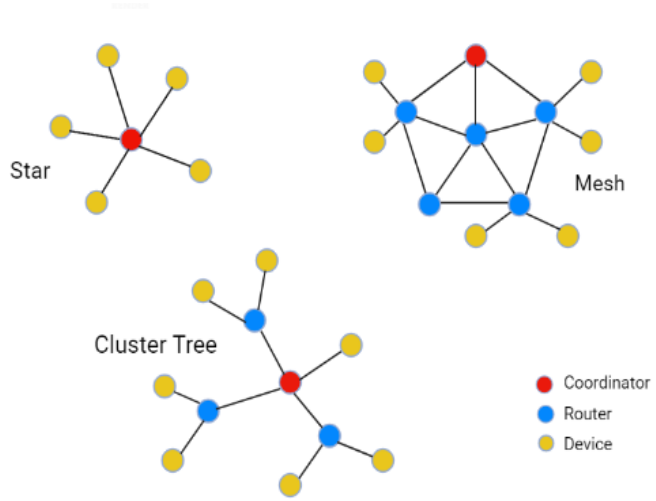

Figure 1.2: Zigbee topologies

A Zigbee network has three types of device roles – coordinator, router and an end device. The coordinator is like the administrator of the network and there should at least be one coordinator in the network. It sets up the network and acts like a bridge and the root of the network. It is responsible for performing data transfer operations, storing and handling information, all the permissions and device accesses are set at the coordinator. The coordinator is supported by the routers that repeat the signal and act as intermediary devices by passing the message to the devices. An end device is reduced function device and does not repeat or forward the signal. These devices do not talk to each and can be anything from a door to CCTV cameras.

1.2.2. Z-Wave

Z-Wave is based on IEEE 802.15.4 standard and operates in sub-GHz (800 – 900 MHz) band (868 MHz in Europe and 908 MHz in United States) [26] which makes it impervious to interference from many other wireless technologies. It supports data rate of up to 100 Kbits/s and provides a coverage of up to 100 meters. It supports mesh topology and while that improves the robustness of the connection, it also drains the battery much faster from the nodes.

The Z-Wave network consists of two basic types of devices – Controllers and Slaves. Controller devices are the devices that control the other nodes in the network. They initiate the control commands and send the commands to other nodes. A controller has the routing table for the entire network and it can communicate with all the nodes. There are two types of controllers, primary and secondary, with the primary controller responsible for setting up the network. Primary controller is responsible for the inclusion of other nodes to the network and can also exclude nodes. The slave devices are the nodes that receive the command and execute them. They do not talk to each unless instructed to do so by the controller. These nodes act as repeaters and transmit the command to the nodes not directly accessible to the controllers. The topology of the Z-Wave network can be seen in Figure 1.3.

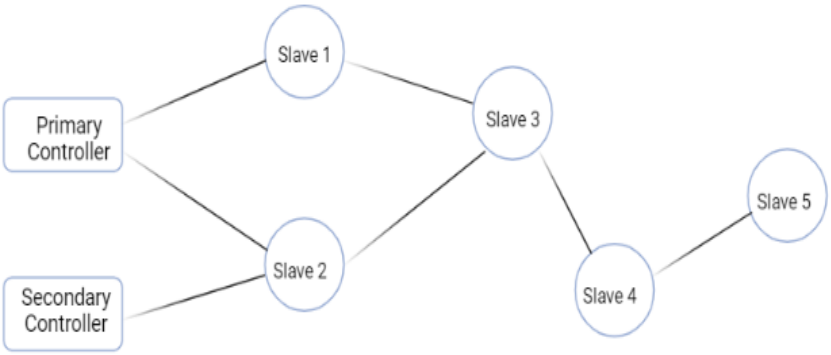

Figure 1.3: Z-Wave Network

In the Z-Wave protocol stack, Figure 1.4, PHY layer is responsible for modulation and channel assignments. MAC layer is responsible for controlling the medium between the nodes based on collision avoidance algorithm. The Transport layer takes care of transmission/re-transmission and reception of frames, ensuring error-free communication in the network. Network layer is responsible for routing and network organisation. Application layer is responsible for defining which applications handle what messages in order to accomplish a particular task.

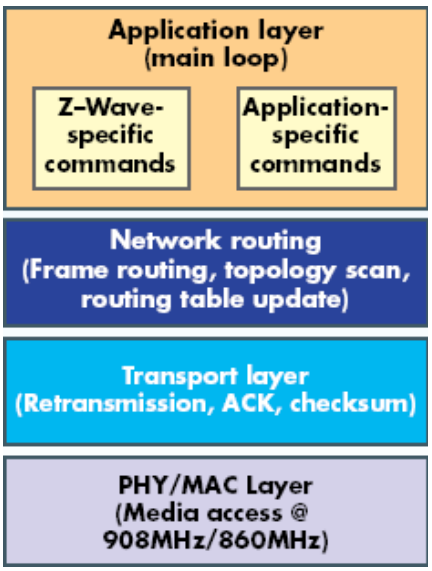

Figure 1.4: Z-Wave Protocol Stack

(Zhidong Deng, 2008)

1.2.3. Bluetooth Low Energy (BLE)

Bluetooth Low Energy (BLE) [27], also referred to as “Bluetooth Smart”, is a standard defined by Bluetooth Special Interest Group (SIG) with a focus on low energy. It operates in 2.4 GHz ISM band and supports data rates from 125 Kbps to 2 Mbps and provides a coverage range of up to 100 meters. BLE framework consists of 40 frequency channels and is separated by 2MHz in order to save energy and provide higher data rates. Among these 40 channels, 3 are reserved for advertisement and the rest are data channels.

BLE supports multiple network topologies as can be seen in Figure 1.5. BLE features two types of devices – central (client) and peripheral (server). Central device is a device that initiates the commands and accepts the response from the peripheral devices. The peripheral device is the device that receives the commands from the client and returns the response corresponding to those commands. In BLE, the data is sent in small packets with the maximum data size of 27 bytes allowed for transmission. The difference between conventional Bluetooth and BLE is that conventional Bluetooth is suitable for applications that require continuous data streaming while BLE is suited for applications requiring periodic data transfer and thus reducing the battery usage.

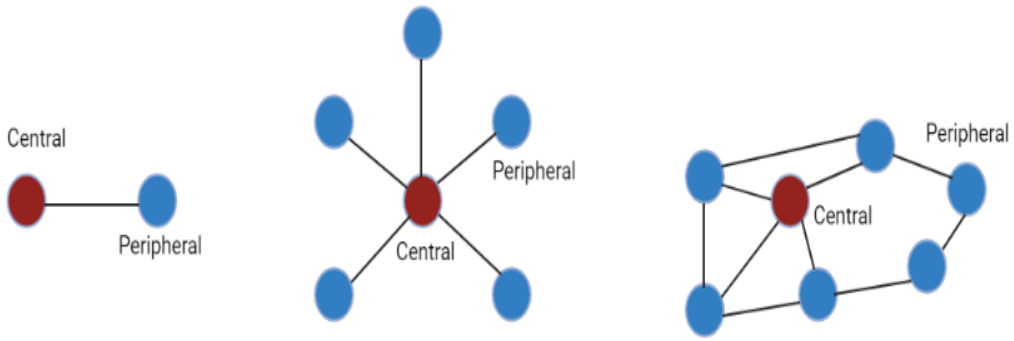

Figure 1.5: BLE topologies

1.3. Low Power Wide Area Networks (LPWANs)

LPWAN has gained prominence over LR-WPAN due to the fact that LPWAN provide connectivity over long range while providing low power consumption. These networks are low cost, operate in unlicensed sub-GHz bands and use the star topology.

1.3.1. LoRaWAN

LoRaWAN is a communication protocol and the system architecture for the network and deals with MAC layer. LoRaWAN specification is a Low Power Wide Area Network (LPWAN) protocol designed for IoT. It implements a star-of-stars topology which makes the most sense for preserving battery lifetime while achieving the long range communication. The aim is to have devices operating on a battery that lasts for long duration of time (10 years or more). It makes use of ALOHA protocol, adopting pure ALOHA mechanism. Network structure for LoRaWAN can be seen in Figure 1.6.

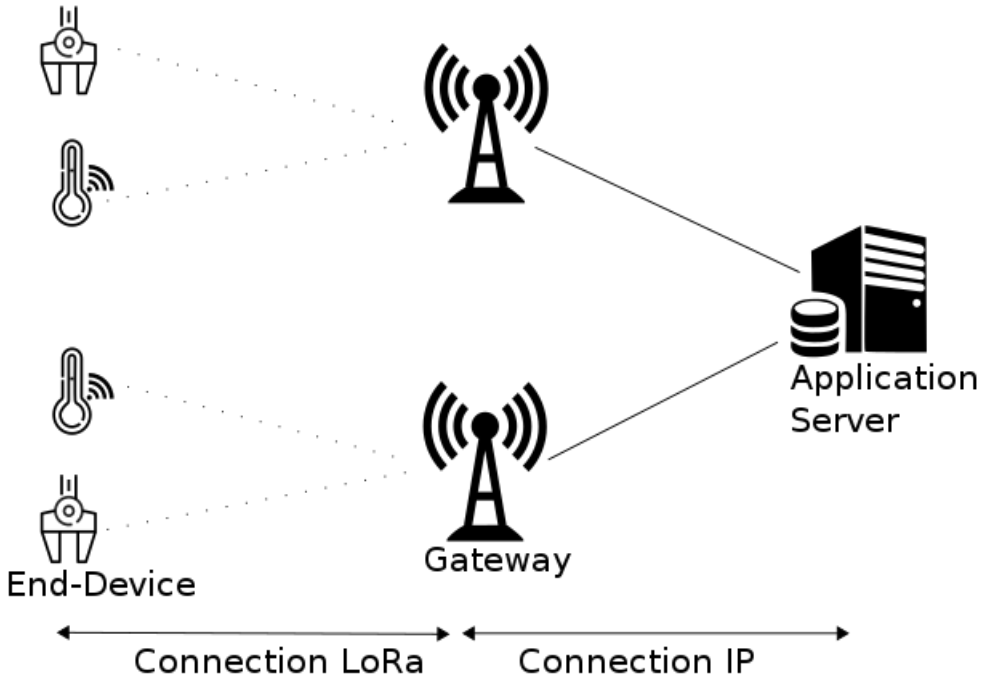

Figure 1.6: Network structure for LoRaWAN

In this topology, the *Gateway (GW)* is responsible for relaying messages from the *End Devices (EDs)* to the *Network Server (NS)* – Uplink and from *NS* to *EDs* – Downlink, the communication is bi-directional. The number of *GWs* in the network can be more than one and the *EDs* do not need to send the data to a particular Gateway. The End Devices transmit data in a fashion where the assumption is that one of the *GWs* will receive it and relay it forward to *NS*. In case duplicate messages are received, *NS* filters them out and if a downlink messages needs to be sent, it selects an appropriate GW to send the message to that *ED*.

In [4] frequency bands in which LoRaWAN operates for different regions are specified. Some of them are given in the Table 1.1.

Table 1.1: Frequency plans for different regions

Region	***Frequency band (MHz)***
Europe	863-870
USA	902-928
China	779-787
Australia	915-928
South Korea	920-923
India	865-867
Russia	864-870

1.3.2. Sigfox

Sigfox [28] is also a LPWAN, employing a star topology, which connects devices while aiming to keep the power consumption low and operating over large distances. Sigfox uses Ultra Narrowband (UNB) technology where signals are sent very infrequently. Sigfox allows 140 uplink messages a day [29] with a size of 12 bytes per message, also allowing 4 downlink messages each being 8 bytes in size. A message can be sent every 10 minutes because of the restrictions Sigfox imposes on its data transmission protocol. The network structure for Sigfox can be seen in Figure 1.7.

A Sigfox message always follows the same cycle. A device wakes up to send a message, a base station receives the message and then send the message to the Sigfox cloud. The Sigfox cloud then sends the message to a customer's backend platform [2].

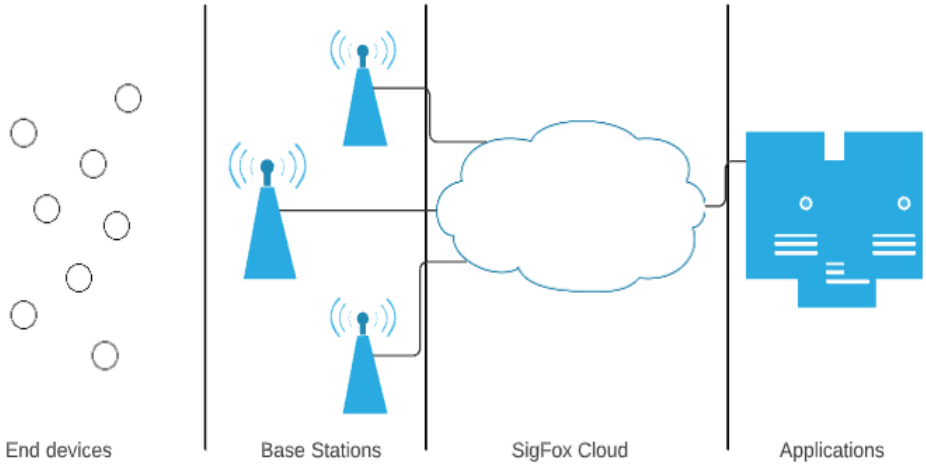

Figure 1.7: Network structure for Sigfox

1.3.3. Weightless

Weightless [30] [31] is a narrowband LPWAN technology and has three versions – Weightless –W, Weightless –N and Weightless –P, all three protocols support different modalities and use cases.

- Weightless –W operates in the TV white space (TVWS) spectrum (470MHz – 790MHz), it takes advantage of the ultra-high frequency (UHF). However the downside is that this frequency might not be available to use everywhere which limits the deployment of this protocol. The data packet size is 10 bytes and data rates vary between 1 kbps to 10 Mbps. Wide range of spreading codes and modulation techniques are supported by this protocol.

- The other variation Weightless –N is an ultra-narrowband protocol much like the Sigfox. It operates in an unlicensed band and uses slotted ALOHA. It only supports unidirectional communication, from end devices to the base station (uplink). The range of 3 km and the maximum data rate of 100 kbps is achieved.

- Weightless–P offers bi-directional communication with support for acknowledgements, uses FDMA/TDMA modulation and occupies 12.5 KHz narrowband channels. The transmit power for uplink and downlink is controlled in an attempt to reduce interference and maintain the highest possible capacity. The maximum achievable data rate and communication range are 100 kbps and 2 Km respectively.

1.3.4. Ingenu

Ingenu (formerly known as On-Ramp Wireless) is based on Random Phase Multiple Access (RPMA), a proprietary technique, and operates in unlicensed ISM bands. It uses a direct sequence spread spectrum (DSSS) modulation and the maximum data rate of 80 kbps is achieved. The use of 2.4 GHz ISM band gives it an advantage as it does not have heavy restrictions regarding duty cycle as the sub-GHz band does. It offers bi-directional communication and to add reliability to the communication, the acknowledged transmission is provided along with the offering secure communication using AES 128-bit encryption. Due to its higher transmission rates, power consumption is more compared to some of the other LPWAN solutions. Ingenu supports star and tree topologies and the payload size of 10 Kbytes and also offers over-the-air updates for devices. The network structure of Ingenu can be seen in Figure 1.8.

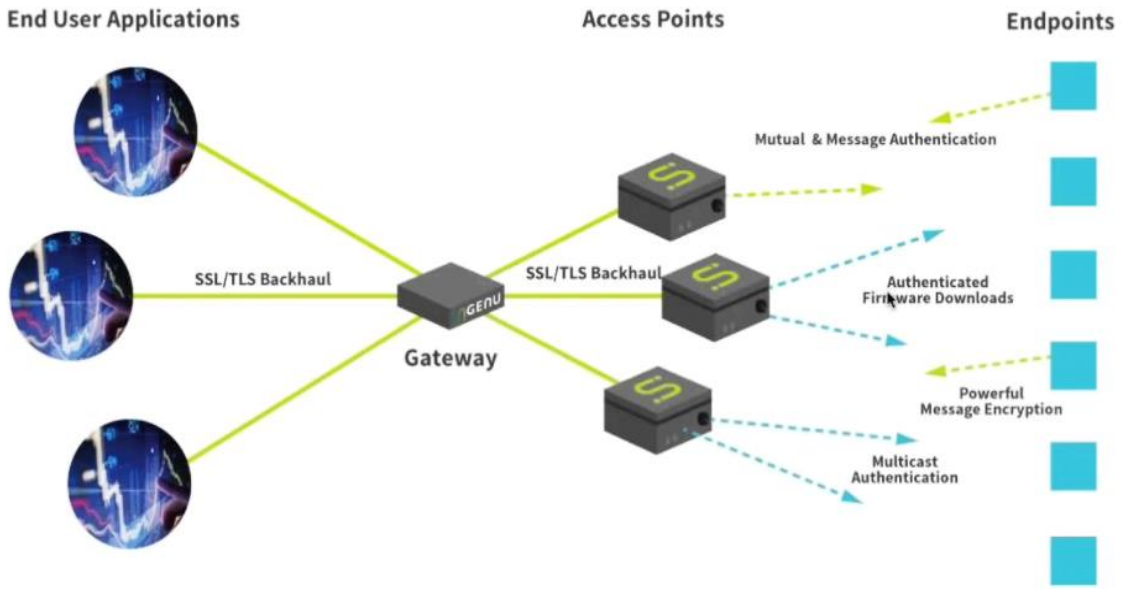

Figure1.8: Ingenu Network Structure

(**Ingenu, 2016**)

1.3.5. Telensa

Telensa is a proprietary ultra-narrowband (UNB) LPWAN technology developed by Telensa and operates in sub-GHz (868 MHz and 915 MHz) unlicensed ISM bands. It offers bi-directional communication with a payload size of 64 Kbytes and provides data rates of 62.5 bps for uplink and 500 bps for downlink transmission. It supports star topology and provides the coverage range of about 2 Km in urban

and 4 Km in rural areas. It has a central management system (CNS) called Telensa PLANet used for end-to-end operations. Currently, Telensa is focused on some smart city applications like smart lighting. The automatic fault detection of CMS makes it possible to reduce the energy consumption and maintenance costs. It features bi-directional unicast and broadcast communications. Telensa, in cooperation with ETSI, is aiming to standardize its technology.

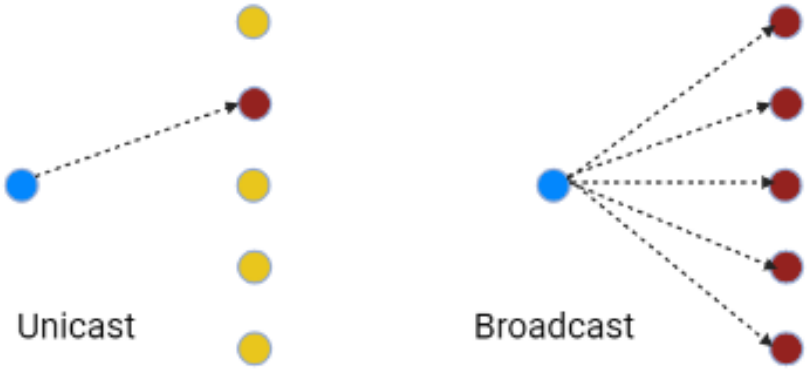

Figure 1.9: Unicast and Broadcast transmission

1.4. Cellular IoT

Cellular IoT will provide the device connectivity to the Internet and will leverage the already existing cellular networks, which is beneficial as the infrastructure is already installed. It offers long range communication and low power consumption while providing higher data rates compared to LRWPAN and LPWAN.

1.4.1. LTE-M

LTE-M is a standard developed by 3GPP and uses licensed spectrum, thus it is able to leverage the existing LTE networks allowing extended coverage. It has the highest bandwidth among other LPWA technology and provides voice support via VoLTE. Conventional LTE offers high data rates at a cost of high power consumption which is not acceptable for the IoT paradigm. So in order to satisfy the needs of IoT network and also be complaint to the LTE specifications, the

data rates are reduced to 1Mbps and the bandwidth is reduced from 20 MHz to 1.4 MHz.

In order to extend the battery life, two new features are adopted by 3GPP, namely extended Discontinuous Reception (eDRX), and Power Saving Mode (PSM). The end devices enter the deep sleep mode for long durations, sometimes days, without losing their network registration. Both aim to reduce the power consumption and extend the battery life. With eDRX, the end device can listen without having to establish a full network connection and thus preserves the end device's power. The end device chooses the length of time it sleeps for instead of the network depending on how long the eDRX cycle has been set. The eDRX cycle could be set depending on the need of the application, for low latency applications shorter time periods can be set. In PSM, the sleep durations are generally longer than eDRX, thus allowing the end devices enter lower power sleep mode than eDRX.

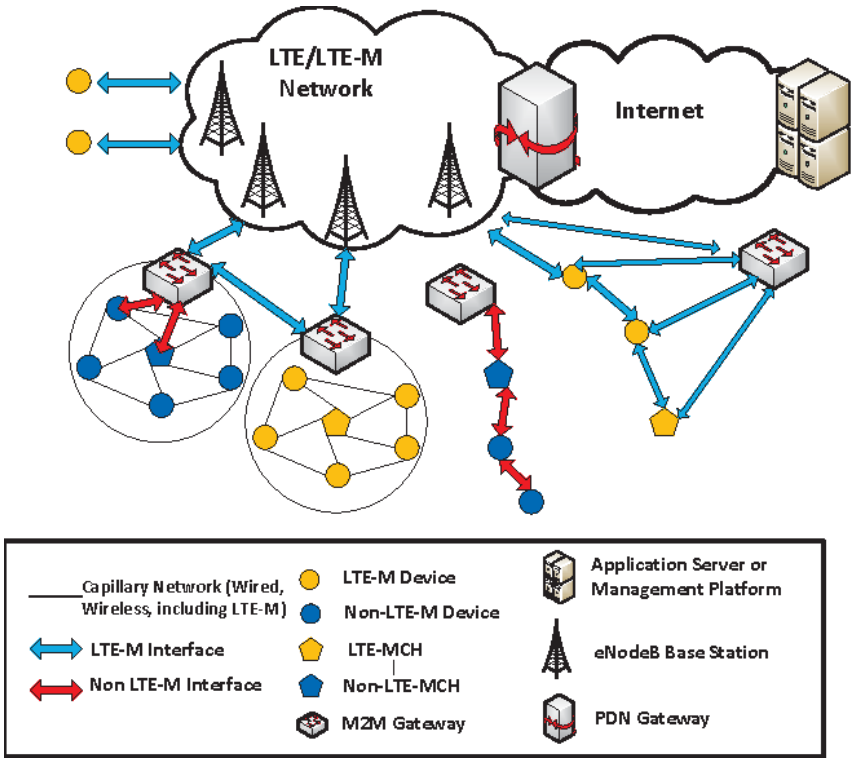

Figure 1.10: LTE-M Network Architecture

(Samir Dawaliby, A. Bradai, Y. Pousset, 2016)

1.4.2. NB-IoT

Narrowband-IoT (NB-IoT) is a wireless communication standard for Internet of Things and it operates over the licensed bands which guarantees quality of service. Thus it makes use of the cellular technologies to connect IoT devices to the internet. NB-IoT can co-exist with 2G, 3G and 4G mobile networks and also benefits from all the security and privacy of mobile networks.

NB-IoT utilizes narrow spectrum bands of 180 KHz, and the data rate peaks at around 250 kbps and it supports Half Duplex FDD mode. Similar to others, a device in NB-IoT is typically in sleep mode and wakes up only when it has to transmit data. The device after transmission remains active for a while before going to idle state and then finally disconnecting.

Chapter 2: LoRa/LoRaWAN Technology

2.1. Overview

LoRa [34] is a modulation scheme utilized for long range communication and is a proprietary protocol developed by Semtech. Due to it being proprietary the information about its implementation is not readily available. However, some of the information has been released by Semtech and also the protocol has been analysed and reverse engineered by the researchers to a point where its implementation has been well understood. It is based on CSS (Chirp Spread Spectrum) modulation technique and it can use one or more channels. It has become the go to technology for IoT networks credit to its ability to provide long range and low power. It operates in the unlicensed ISM band, and uses sub-GHz frequency bands.

2.2. LoRa – Chirp Spread Spectrum

The concept behind CSS is the use of chirps with linearly varying frequency over time to encode the information. An advantage of this method is that timing and frequency offsets between transmitter and receiver are equivalent, greatly reducing the complexity of the receiver design [3]. In Figure 2.1, we have the spectrogram representation of a LoRa signal with horizontal axis representing time and the vertical axis representing frequency. If the chirps are continuously increasing in frequency, they are termed as up-chirps and if they are decreasing in frequency they are termed as down-chirps. The continuously varying frequency also makes it resistant to Doppler Effect. The important parameters to understand it better are Bandwidth (BW), which determines the difference between the maximum and minimum frequency ($f_{\max}$,$f_{\min}$) and the Spreading Factor (*SF*). The starting frequency of the chirp can be any frequency within the Bandwidth and it starts from that frequency and increases linearly, reaching the same frequency back. The number of bits encoded in a symbol is called SF. So, a chirp using spreading factor SF represents 2^{SF} bits, the number of possible starting frequencies for that particular chirp are 2^{SF}.

Using these parameters, SF and BW, the duration of the symbol can be calculated as shown in Eq. 2.1:

$$T_s = \frac{2^{SF}}{BW} \tag{2.1}$$

where,

- BW is the Bandwidth
- SF is the spreading factor

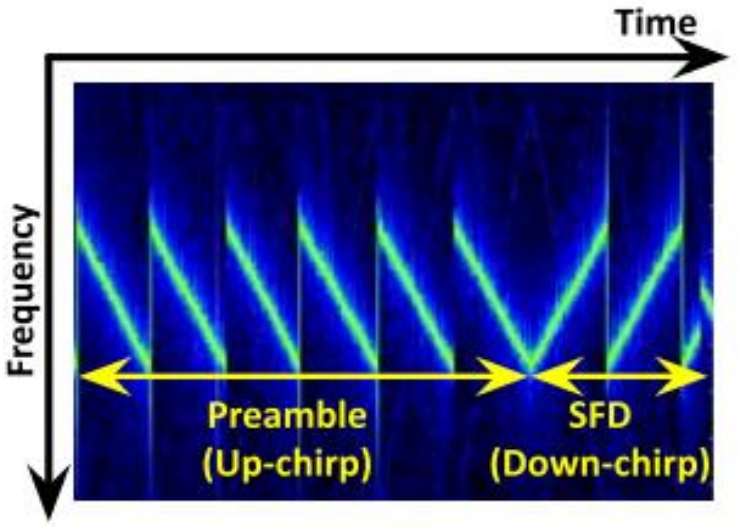

Figure 2.1: Spectrogram representation of a LoRa signal [32]

Table 2.1: Bitrates (bits/s) for different Spreading Factors for BW 125 kHz

SF	R_b (bits/s)
7	*5470*
8	*3125*
9	*1760*
10	*980*
11	*440*
12	*250*

From Equation 2.1, we can conclude that increasing the value of SF by 1 will result in increase in the duration of the symbol by a factor of 2. LoRa has 6 SFs i.e., it can have a value between 7 and 12. Higher SFs increase the coverage area because of the increase in ToA (slower transmission and higher processing gain) with a disadvantage being the reduction in the data rate and more energy consumption. On the contrary larger BW decreases the duration of the symbol and subsequently increases the data rate of the modulation.

Given Equation 2.1, we can now compute the bitrate for the desired values of SF and BW as

$$R_b = SF * \frac{1}{\frac{2^{SF}}{BW}} \tag{2.2}$$

where,

- BW is the bandwidth
- SF is the spreading factor

Table 2.2: SNR values for different spreading factors

SF	***SNR***
7	-7.5 dB
8	-10 dB
9	-12.5 dB
10	-15 dB
11	-17.5 dB
12	-20 dB

The bit rates for different SFs and a BW of 125 kHz can be seen in Table 2.1 [4]. Employing a higher *SF* gives an advantage of achieving better robustness to the

interference. However, the disadvantage being the increased probability of the collisions among the packets sent.

Another important parameter is the receiver sensitivity which is affected by the SF selected for the transmission. The receiver sensitivity is defined as:

$$S = -174 + 10\log_{10}(BW) + NF + SNR \quad dBm \tag{2.3}$$

where,

- *-174* is due to the thermal noise in 1 Hz of bandwidth, in dBm
- *BW* is the receiver bandwidth, in Hz
- *SNR* is the signal to noise ratio, in dB
- *NF* is the receiver Noise Figure, in dB

The noise figure is the amount of noise power added by the RF front-end in the receiver to the thermal noise power from the input of the receiver [5]. The *NF* is fixed for a given hardware implementation. *SNR* values for different spreading factors are shown in Table 2.2 [6].

The sensitivity values for different spreading factors can be seen in Table 2.3 [6]. As the *SF* increases it results in providing better sensitivity.

Table 2.3: Sensitivity threshold for different spreading factors

SF	***S(dBm)***	***S(mW)***
7	-124	$4 * 10^{-13}$
8	-127	$2 * 10^{-13}$
9	-130	$1 * 10^{-13}$
10	-133	$5 * 10^{-14}$
11	-135	$3.2 * 10^{-14}$
12	-137	$2 * 10^{-14}$

Another important and powerful capability of LoRa modulation is that the spreading factors are orthogonal. This enables multiple signals to be transmitted on the same channel concurrently without interfering. The receiver correctly detects the packets employing different spreading factors, the only condition being that the two spreading factors should not be the same. This feature allows to significantly improve the network efficiency and throughput.

2.3. LoRaWAN

We briefly touched on LoRaWAN in Chapter 1, but now we will take a deeper look into this protocol. In [7], LoRaWAN is described by the LoRa Alliance as:

The LoRaWAN® specification is a Low Power, Wide Area (LPWA) networking protocol designed to wirelessly connect battery operated 'things' to the internet in regional, national or global networks, and targets key Internet of Things (IoT) requirements such as bi-directional communication, end-to-end security, mobility and localization services.

2.3.1. Network Topology

LoRaWAN employs a star-of-stars topology, with important components being *End Devices (EDs)*, *Gateways (GWs)* and *Network Server (NS). End Devices* are the sensors that send and receive the packets from the *Gateways* and a certain *ED* does not have to be allocated to only one *GW* but on the contrary can send the packets to more than one *GWs.* The topology is illustrated in Figure 2.2, the *GWs* then relay the packets forward to the *NS. Network Server* then acts as a bridge between these components and the *Application Server (AS).*

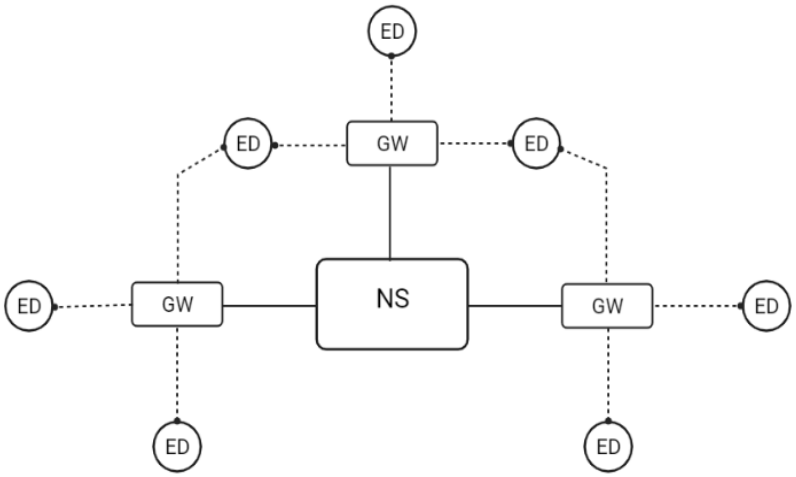

Figure 2.2: LoRaWAN network topology

2.3.2. Device Classes

According to [8], LoRaWAN specifies three categories of devices (Class A, B and C), with the minimum requirement being that all the LoRaWAN devices must at least have Class A functionality. The LoRaWAN classes are illustrated in the Figure 2.3.

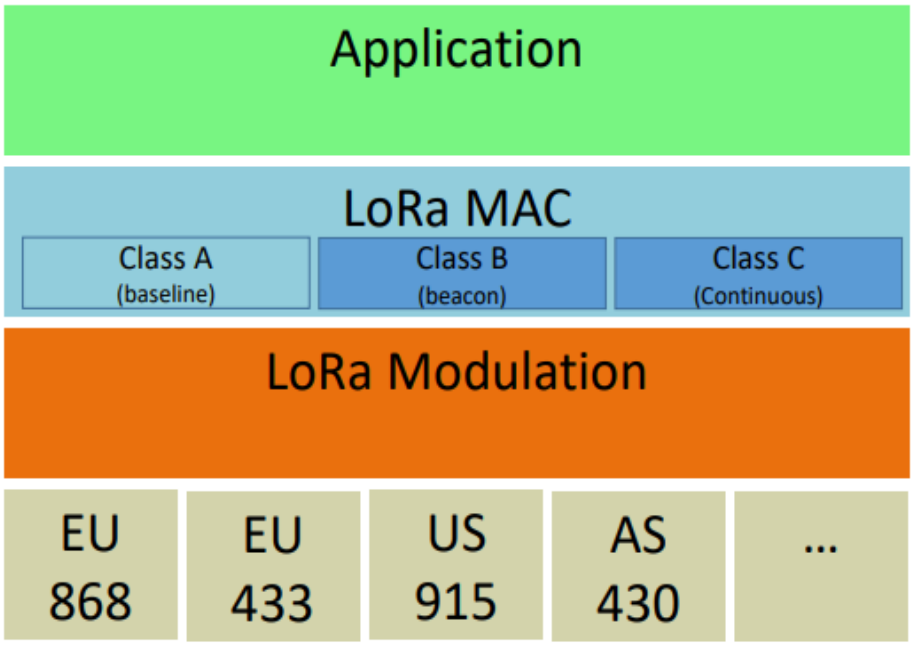

Figure 2.3: LoRaWAN Classes

The different classes are defined below:

- **Class A:** This is default class and must be supported by all the end-devices. End Devices use ALOHA protocol for the bi-directional communications and the communication is always initiated by the end-device. Both uplink and downlink transmissions take place on the same channel, where after every uplink transmission two downlink receive windows (RX_1 and RX_2) are opened, in case any message needs to be sent from the *NS* to the *ED*. The downlink transmission must happen within the time frame of these two windows. Downlink transmission outside of these two windows is not possible. In case a downlink transmission is required at any other time, the server has to wait until the next uplink transmission. This class is employed by the devices where there is need to have low power consumption as these devices are mostly in the sleep mode and only wake up when there is a need for an uplink transmission.

- **Class B:** In addition to the functionality of Class A devices, Class B devices also have more receive slots and they do so by opening receive windows at scheduled time slots. The opening of the windows at the scheduled time slots is carried out by a time synchronised beacon from the Gateway, which notifies the Network Server about the listening status of the end-devices. Class B has higher power consumption than Class A.

- **Class C:** The end-devices of this class are always in the reception mode and have open receive windows except when transmitting. This class is suitable for devices with no strict energy constraints and continuous power is available and provides low latency communication. Class C has the most power consumption among all the classes.

2.3.3. LoRa Physical Message Formats

A physical frame format both for Uplink and Downlink messages are specified by Semtech and implemented in transmitters and receivers. Spreading factor and Bandwidth remain constant for a message frame. LoRa frame starts with a preamble followed by a header and ends with cyclic redundancy check. The difference between two PHY formats, uplink and downlink is that uplink contains a *CRC* field.

The preamble begins with a sequence of upchirps for the entire frequency band and the last two upchirps have the sync word encoded in them. Sync word is useful in differentiating the LoRa networks operating in the same frequency bands. An end device will not listen to the transmission if the decoded sync word does not match its configured sync word. The preamble varies between regions and for Europe LoRa uses 8 symbols. The *PHYPayload* can be of variable length, ranging from 0 bytes to a maximum of 255 bytes and is sent after the header. A schematic summary of the uplink PHY format can be seen in Figure 2.4. Uplink messages are sent by *EDs* to the Network Server.

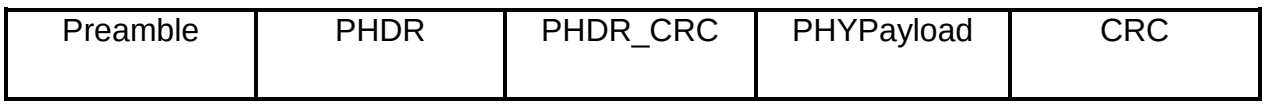

Figure 2.4: Uplink PHY structure

The downlink message is sent by the Network Server to the *EDs*. The Downlink PHY structure is depicted in Figure 2.5, we can see the difference being the absence of the *CRC* field.

Preamble	PHDR	PHDR_CRC	PHYPayload

Figure 2.5: Downlink PHY structure

Some other important parameters and operations specified by LoRa are:

- **Time on air:** This is the time it takes to transmit a LoRa message. In case the payload increases, time on air increases as well
- **Coding Rate:** In order to further improve the robustness of the network cyclic error coding is used to perform forward error correction (FEC). LoRa uses Hamming codes for FEC. The offered code rates are 4/5, 4/6, 4/7, 4/8.

The packet time on air (ToA) can be calculated with the equation given below:

$$T_{packet} = T_{preamble} + T_{payload} \quad (2.4)$$

where $T_{preamble}$ represents the time to transmit the preamble and $T_{payload}$, the time to transmit the payload.

The time to transmit preamble can be calculated as:

$$T_{preamble} = (n_{preamble} + 4.25) \cdot T_s \quad (2.5)$$

where $n_{preamble}$ is the preamble length and is a configurable parameter.

The expression for transmit time of the payload is:

$$T_{payload} = n_{payload} \cdot T_s \quad (2.6)$$

To calculate $n_{payload}$ we use the following equation:

$$n_{\text{payload}} = 8 + \max(ceil\left[\frac{8PL - 4SF + 28 + 16CRC - 20IH}{4(SF - 2DE)}\right](CR + 4), 0) \quad (2.7)$$

where,

- PL is the number of bytes of payload
- SF is the spreading factor
- IH can be 0 when the PHY header is not enabled, or 1 when the PHY header is enabled
- DE =1 indicates the use of low rate optimization whereas DE = 0 indicates that low rate optimization is disabled
- CRC indicates the presence of the payload, CRC = 1 shows the field is present and CRC = 0 indicates its absence
- CR is the coding rate, depicts the number of added parity bits.

The $ceil$ function indicates that the part of the equation within the square brackets should be rounded up to the next integer value. The $\max$ function compares the $ceil$ function result and returns the highest value between the result and 0.

2.3.4. MAC Message Formats

The PHY payload contains the MAC packets. The structure of the PHY payload is illustrated in Figure 2.5. It starts with the MAC header (MHDR), which provides the information about the LoRaWAN version of the device and specifies the message type.

MHDR	MACPayload	MIC

Figure 2.6: PHYPayload

The types of messages are:

- Join messages are the packets sent by the device in an attempt to join the network. This procedure of joining is always initiated by the device.

- Data messages give the information whether it is uplink or downlink message. Also, this message has two types, confirmed or unconfirmed which states whether an acknowledgement is needed or not by the message.

- Proprietary messages can be used to incorporate non-standard message format functionalities and must be used among devices that have a common understanding of the proprietary extensions.

The MACPayload consists of three fields Frame header (FHDR), Frame port (FPort) and Frame payload. The structure of the MACPayload is illustrated in the Figure 2.6. MACPayload has a dynamic size as opposed to the fixed size of MHDR and MIC.

Figure 2.7: MACPayload

Frame payload contains the data which can be MAC commands or the application data. The Frame port indicates what Frame payload contains, a value of 0 tells that FRMPayload only contains MAC commands. Ports 1 to 223 are kept to be used by the applications and are thus application specific, while Port 224 is only intended for LoRaWAN MAC layer test protocol. The remaining ports are reserved for standardised application extension with a view of using them in the future.

The Framer header consists of short device address (DevAddr), Frame Control (FCtrl), Frame Counter (FCnt) and Frame Options (FOpts). The Frame header can be seen from the Figure 2.7.

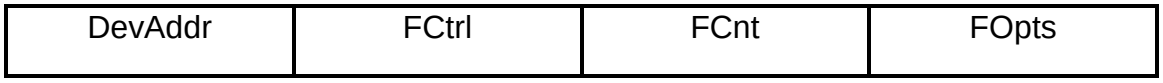

Figure 2.8: Frame Header

The DevAddr is 4 bytes and is used to identify the end device in the network. Frame Control is 1 byte and has various fields, it is responsible for implementing Adaptive Data Rate (ADR). ADR is a feature to allow end devices to use any of the available data rates and transmission power, by doing this end devices can optimize the transmission by selecting a suitable Spreading Factor. In case the ADR is set, the *NS* controls the data rate and the transmission power of the end device by sending the appropriate MAC commands. If ADR is not set, the *NS* does not control the data rates and the transmission power irrespective of the received signal quality. In addition to this feature, it is also has an Acknowledgement (ACK) bit. In case the *NS* receives a confirmed data messages from the end device, it has to respond back with an ACK during one of the receive windows. The frame pending bit in Frame Control is only used in downlink and depicts that network has more data to be sent and thus asking the end device to open the receive windows by sending the uplink transmission. The 2 byte Frame counter field keeps track of the number of frames sent by end devices to the *NS* (FCntUp) and from the *NS* to the end devices (FCntDown). The Frame options

field contains MAC command and has a maximum length of 15 bytes. In case the MAC commands are present in the payload field as well as frame options field, the end device ignores the frame. Encryption of FOpts must take place before the message integrity check (MIC) is calculated, the encryption used is based on IEEE 802.15.4 standard [9] using AES.

2.3.5. MAC Commands

A set of MAC commands is exchanged between the end devices and the *NS* for the purpose of network administration, which comprises of making modifications in communication parameters. The features of these MAC commands are:

- Link check: This is used by the end device to confirm its connectivity status with the network. The response from the *NS* is the received signal power which determines the quality of reception.
- Duty cycle: To have a control over the aggregated transmit time of the end device.
- ADR request: The *NS* can ask the end device to make changes in the data rate and transmit power, thus effectively changing the *SF* and the end device can acknowledge the request.
- Reception parameters setup: Setting the receive windows parameters.
- Device status: The *NS* asks the end device about the information regarding its battery level and demodulation margin.
- New channel: To create or modify the radio channel.
- Reception timing: To set up the timing of the reception slots for the end devices.
- Transmission parameters setup: Based on the regulations of the region, the *NS* sets the maximum allowed dwell time and Max EIRP of the end device.

The end device only replies once to the MAC commands it receives. In case the reply is lost, and the next uplink received does not contain the answer, the *NS* has to send the command again.

2.3.6. Device Activation

The end devices need to be registered with the network before being able to exchange messages. This process is known as activation, with two ways provided by LoRaWAN standard to achieve it. These two ways being: Over-The-Air Activation (OTAA) and Activation By Personalization (ABP).

2.3.6.1. Over The Air Activation:

The end devices go through a join procedure with the network and are assigned device address and security keys are obtained as well. This method is the most secure because the device address assigned is dynamic.

The join procedure consists of following exchanges between the end device and the network:

- Join-request
- Join-accept

Before the activation process begins the JoinEUI and DevEUI must be stored in the end device. JoinEUI is 64 bit global application ID in IEEE EUI64 address space and is unique to every Join Server and thus helps in identifying a particular network. The Join Server aids in the process of Join procedure and for obtaining the session keys. DevEUI is a 64 bit global end device ID in IEEE EUI64 address space and is unique to every end device. It helps in identifying the end device when it roams across networks. The end device should also possess AppKey and NwkKey, which are AES-128 root keys. While JoinEUI and DevEUI are visible to everyone, the AppKey and NwkKey are secret keys and are never sent over the network.

The Join-request is sent by the end device and consists of three fields: JoinEUI, DevEUI and DevNonce. The end device sends the Join-request using one of the specified join channels and one or more gateways in the network relay the message to the network server. While sending the request the end devices can employ any data rate and the joining channels are region specific.

The Network Server sends the Join-accept message to the end device indicating the success of the procedure. This message is sent as a normal downlink message and is encrypted with NwkKey. The end device then generates network session keys and application session keys, the network session keys are derived from NwkKey.

2.3.6.2. Activation By Personalization

The end devices have device address and Network and Application keys stored in them, thus by-passing the join procedure. Activation By Personalization is less secure and also has a downside of being tied to a specific network and requires manual change of keys in the device to be able to switch the network. The device already has the required information to connect to a specific network when it is started. The same Network keys and device address are stored in the Network Server and the Application keys are stored in the Application Server.

Chapter 3: State of the Art

In this chapter we discuss the importance of knowing the performance and scalability of a network with a focus on LoRaWAN and how the performance is measured. We also go through some of the past works done in this field and their process to achieve this goal through various metrics.

3.1. Overview

Most LPWAN technologies claim to have the capacity to connect massive number of devices, in the order of tens of thousands, to each other and to the Internet. It becomes vital to determine the validity of such claims before deploying these networks in the field. We specifically focus here on LoRaWAN and its challenges regarding performance and scalability. It is important to know how the network will behave with the increase in demand (i.e. increase in the number of devices) and how easily can the capacity be increased based on the requirements of the connected or connecting new devices. As the aim is to cover a large geographical area, the devices will need to share the wireless medium, which raises the question of how many devices can be supported in a certain area while maintaining the QoS requirements.

Some of the essential parameters used to monitor network performance are:

- Throughput
- Latency
- Packet loss
- Bandwidth

In the next section, we take a look at some of the studies that have been conducted about LoRa/LoRaWAN in the past focusing on the parameters listed above and more. Furthermore, these studies also determine the factors impacting the network performance, such as use of multiple gateways (different approaches to their placements in the network), SF assignment and inter-technology interference.

3.2. Scalability analysis of large-scale LoRaWAN networks in ns-3

In [10], the authors have studied the impact of confirmed and unconfirmed messages on the scalability of the network. They built an error model for LoRa modulation corresponding to different coding rates and spreading factors. The

simulations were run using ns-3 simulator and for multiple gateways (1, 2 and 4). In case of one gateway it is positioned at the centre of the disc with radius 6100m. In case of two gateways, they are positioned one radius apart on a diameter line of the disc. In case of four gateways, they are positioned on the corners of a square which is centred on the origin and has a diagonal equal to the radius of the disc.

The assignment of the Spreading Factors (SF) was done using different strategies:

1. Random: Assign the SF to the end devices according to the uniform random distribution.
2. Fixed: Assign the same SF to all the devices.
3. PER: Set a threshold for packet error ratio and assign the SF to the end devices accordingly.

The conclusion reached by the authors after applying all the strategies was that the PER strategy had the best performance in terms of the Packet Delivery Ratio.

The SF allocated to the end devices based on PER strategy which is as it should be, with higher SF's being allotted to the devices further away from the gateway. They drew the conclusion that PDR increases as the number of the gateways are increased but it does not completely eliminate the problem.

3.3. A LoRaWAN module for ns-3: implementation and evaluation

In [11], the authors have studied the impact of multiple gateways on the performance of the network. The work is carried out with a module that supports distributed gateways.

To carry out the simulations the authors chose three different scenarios:

1. Scenario 1: Simple network topology with nodes in a circle and then send data to a central gateway. The nodes transmit unconfirmed data to the network server and do not wait for the acknowledgement.
2. Scenario 2: This scenario is similar to the first one but with seven gateways being employed in the simulation.
3. Scenario 3: Again similar to the Scenario 1 but this time the nodes transmit confirmed messages.

The findings for the Scenario 1 showed that PER is low closer to the gateway but the performance of the network decreases as the distance from the gateway increases and as the density of the nodes increases as well. The Scenario 2 showed that PER followed almost the same trend as in the Scenario 1 but after a certain point (>550 m), the PER decreased due to the presence of other gateways as they were able to receive the packets from those nodes. The Scenario 3 depicted that PER for small number of nodes (100 in this case) is

always zero, but as the number of nodes increase the PER increases drastically thus deteriorating the channel. This study showed that in the scenarios where the nodes require an acknowledgement, the performance of the network degrades with the densification of the network. Hence, this study showed that acknowledgements do not scale in LoRaWAN.

3.4. TS-LoRa: Time-slotted LoRaWAN for the Industrial Internet of Things

In [12], the authors have proposed a Time slotted approach to tackle overheads by allowing devices to self-organise and determine their slot positions in a frame autonomously. In Time slotted LoRa, in order to avoid collisions, transmissions are performed during specific time slots using a time division mechanism. Structure of the frame used in this approach consists of slots for different transmissions as well as a slot for acknowledgements.

The experimental setup consists of two gateways, one responsible for the joining requests and the other used solely for data collection and transmission of the acknowledgements. A simulation with two nodes, one close to the gateway with LOS and the other further away, non-LOS was carried out and PDR was measured. The results showed that even the furthest node achieved more than 99.8% PDR, which showed for a better outcome than the traditional ALOHA based approach.

Another simulation where the acknowledgements were considered was carried out and PDR and energy consumption for TS-LoRa and LoRaWAN were measured for variable number of nodes. The results showed PDR for TS-LoRa close to 99% and also the energy consumption was lower than LoRaWAN. It was also concluded that the lost packets in LoRaWAN increased linearly with an increase in the number of nodes due to massive number of collisions. However, the lost packets in TS-LoRa were due to path loss rather than the collisions. Hence, this study concluded that time slotted approach shows for better performance than the traditional approach.

3.5. Optimum LoRaWAN Configuration under Wi-SUN Interference

In [13], performance of a LoRaWAN network was studied while taking into account the inter technology interference from Wireless Smart Utility Networks (Wi-SUN). The authors have proposed scenarios to determine best LoRaWAN configurations targeting a minimum reliability level.

Two scenarios were carried out:

1. Maximizing the number of nodes
2. Maximizing the coverage area

While carrying out these scenarios, different reliability targets were set and the packet generation time was changed as well. For the first scenario, the radius was taken as an input and results showed the maximum number of nodes that could be achieved under those conditions. Similarly, for the second scenario, the number of nodes were changed and the results depicted the maximum area that would be under coverage while respecting the predefined set targets. The aim of the study was to find a trade-off between network load and the coverage area.

3.6. LoRa Beyond ALOHA: An Investigation of Alternative Random Access Protocols

In [14], the performance of different protocols is studied and the comparison between P-ALOHA, S-ALOHA and NP-CSMA is carried out. The authors have studied the impact of interference on the performance of the network and the study of various parameters.

One of the simulations performed was to plot the coverage probability of above mentioned three protocols. The set up for this simulation had nodes at a distance of 3 and 6 km from the gateway and the number of nodes were set to 3000. The results showed that while the coverage probability decreased with an increase in the number of nodes, S-ALOHA performed better than the other two and offered better scalability.
Furthermore, the simulation to study energy efficiency of these protocols was performed. For CSMA, three detection values for detection threshold were set, that is the packets with those power levels will be detected. The values set as threshold were -150dB, -140dB and -130dB. The results of this simulation showed that S-ALOHA performed better than P-ALOHA but CSMA (-150dB) outperformed both S-ALOHA and P-ALOHA. While computing the mean energy efficiency, the performance of CSMA and S-ALOHA were comparable.

The simulation to compute throughput for SF8 and SF12 with the number of nodes set to 6000 was performed. For SF8 CSMA performed the best with its performance going down with more stringent threshold values and S-ALOHA outperformed P-ALOHA. For SF12 the performance of S-ALOHA was above all, when taking the power capture into consideration

Chapter 4: Evaluation and results

4.1. Overview

In order to model our experiments, we first define the metrics that we use in this work. The aim of this work is to determine the actual capacity of a LoRa/LoRaWAN network. Capacity of a network can be defined as the maximum amount of data that a network can handle at a given time. Throughput (often referred to as actual capacity in this work) is the actual amount of data transferred in the network.

We then perform various simulations using ns-3 to test the LoRaWAN network for validation purposes and get the results of parameters like the network throughput. To perform these simulations we use the LoRa module already available in ns-3 [22].

4.2. Installation and validation

The ns-3 [21] is one of the most widely used network simulators. The module we use in this work is available at [22]. This module is widely used for research on LoRa/LoRaWAN technology. We use this tool to perform numerous simulations and evaluate different parameters.

4.2.1. Procedure to install ns-3

Before the installation of ns-3 and the LoRa/LoRaWAN module, we make sure that all the operating system packages are upgraded and up to date. We execute the following two commands in the terminal to achieve it.

```
sudo apt update
sudo apt upgrade
```

To install the ns-3 and the LoRa/LoRaWAN module, we need to run the following command, this will allow us to make use of the module to run the simulations.

```
git clone https://github.com/nsnam/ns-3-dev-git ns-3
git clone https://github.com/signetlabdei/lorawan ns3/src/lorawan
```

Once the installation of ns-3 and LoRa/LoRaWAN module is complete, we now configure and build ns-3.

```
./waf configure --enable-tests --enable-examples
```

This compilation returns results as seen below:

```
kazim@kazim-VirtualBox:~$ cd ns-3/
kazim@kazim-VirtualBox:~/ns-3$ ./waf configure --enable-tests --enable-examples
Setting top to                           : /home/kazim/ns-3
Setting out to                           : /home/kazim/ns-3/build
Checking for 'gcc' (C compiler)          : /usr/bin/gcc
Checking for cc version                  : 9.3.0
Checking for 'g++' (C++ compiler)        : /usr/bin/g++
Checking for compilation flag -Wl,--soname=foo support : ok
Checking for compilation flag -std=c++11 support       : ok
'configure' finished successfully (11.580s)
```

Figure 4.1: Configuring ns-3

Then for building, compiling and installing the modules, we use the following command:

```
./waf build
```

The results should look like the following:

```
kazim@kazim-VirtualBox:~/ns-3$ ./waf build
Waf: Entering directory `/home/kazim/ns-3/build'
Waf: Leaving directory `/home/kazim/ns-3/build'
Build commands will be stored in build/compile_commands.json
'build' finished successfully (2.365s)

Modules built:
buildings                 config-store              core
energy                    lorawan (no Python)       mobility
network                   point-to-point            propagation
stats
```

Figure 4.2: ns-3 modules

To test that the environment has been built correctly, we will now run the tests and generate the results. We do that by running the following command.

```
./test.py -s lorawan
```

If it returns that the lorawan test suite passed, that would mean that it was successfully built and is ready to use.

```
Modules built:
buildings                 config-store              core
energy                    lorawan (no Python)       mobility
network                   point-to-point            propagation
stats

Modules not built (see ns-3 tutorial for explanation):
brite                     click                     dpdk-net-device
mpi                       openflow                  visualizer

[1/1] PASS: TestSuite lorawan
1 of 1 tests passed (1 passed, 0 skipped, 0 failed, 0 crashed, 0 valgrind error
s)
```

Figure 4.3: Verification of built modules

After the test returns the pass, the modules built are shown and now various simulations can be run and results can be gathered for further analysis. We now move to the validation of the LoRaWAN module.

4.2.2. ns-3 LoRaWAN module validation

In Chapter 2, we mentioned that Class A end devices use the ALOHA protocol for communication. In an ideal scenario, there will be no collisions among the packets in the network and the throughput achieved would be equal to 1. However, this becomes impossible to achieve because the devices cannot be perfectly synchronised in a network. So, the expected value of the throughput (S) is expected to be less than 1 (S<1). In the case of LoRaWAN, the throughput is expected to follow the shape of ALOHA medium access protocol as validated by the authors in [33].

4.2.2.1. Analytical model

ALOHA or pure ALOHA operates on a simple rule, if a user has data to send, it sends it. In case a collision occurs, user waits for a random period of time and then re-sends the data again. In order to assess the performance of ALOHA, throughput (S), rate of successful transmissions, needs to be investigated. G (Erlang) refers to average number of transmission attempts in a frame-time (T), time required to transmit one frame on the channel. The throughput is then given by the equation below:

$$S = G * P \tag{4.1}$$

where,

- P is the probability of no collision

Probability of X transmission attempts in a frame time is given by

$$P_X = G^X * \frac{e^{-G}}{X!} \quad (4.2)$$

For a probability that at any particular period only one node transmits

$$P_{X=1} = G * e^{-G} \quad (4.3)$$

Also the probability that no other starts transmission during this period

$$P_{X=0} = 1 * e^{-G} \quad (4.4)$$

For a successful transmission both (3.3) and (3.4) have to occur simultaneously, thus resulting in

$$P = Ge^{-G} * e^{-G} \quad (4.5)$$

Therefore, throughput (S) from Equation 3.1 can be written as

$$S = G * e^{-2G} \quad (4.6)$$

Maximum throughput achieved using ALOHA is obtained by taking a derivative of throughput (S) with respect to load (G). We obtain the value for G_{max} by finding the minimum of the aforementioned derivative, we get $G_{max} = 0.5$. We can then obtain the value for S_{max} (maximum throughput) by substituting the value of G_{max} in Equation 4.6 and we get $S_{max} = 0.1839$.

4.2.2.2. Validation using simulation

The LoRaWAN module is run and tested, in order to verify if the results match the expected outcomes from the aforementioned model. The simulations are run to obtain the result for throughput of the network.

We run the simulations for *N = 2000* end devices in a simulation area with radius *R = 1000 m.* The GW is located at the centre of our simulation area, with the

centre located at the origin *(0, 0)*. All the EDs are assigned SF8 and are thus transmitting with the same data rate. The simulations are run multiple times to compute the mean and standard deviation of the packets received successfully. The validity of the LoRaWAN module can be confirmed if the results of the simulations are same as the results of the analytical model. Figure 4.4 illustrates the results from the analytical model and the simulations. We can see both curves follow the same trend, thus validating the LoRa/LoRaWAN module. The difference in the results as the load increases can be explained due to an important feature of LoRaWAN called 'capture effect'. Capture effect allows the possibility of the correct reception of a packet even if it collides with another packet in time but has slightly higher power than the other one. In this case both the packets are not lost as opposed to the assumptions made in the theoretical approach. The shaded region depicts the standard deviation on either side of the throughput curve.

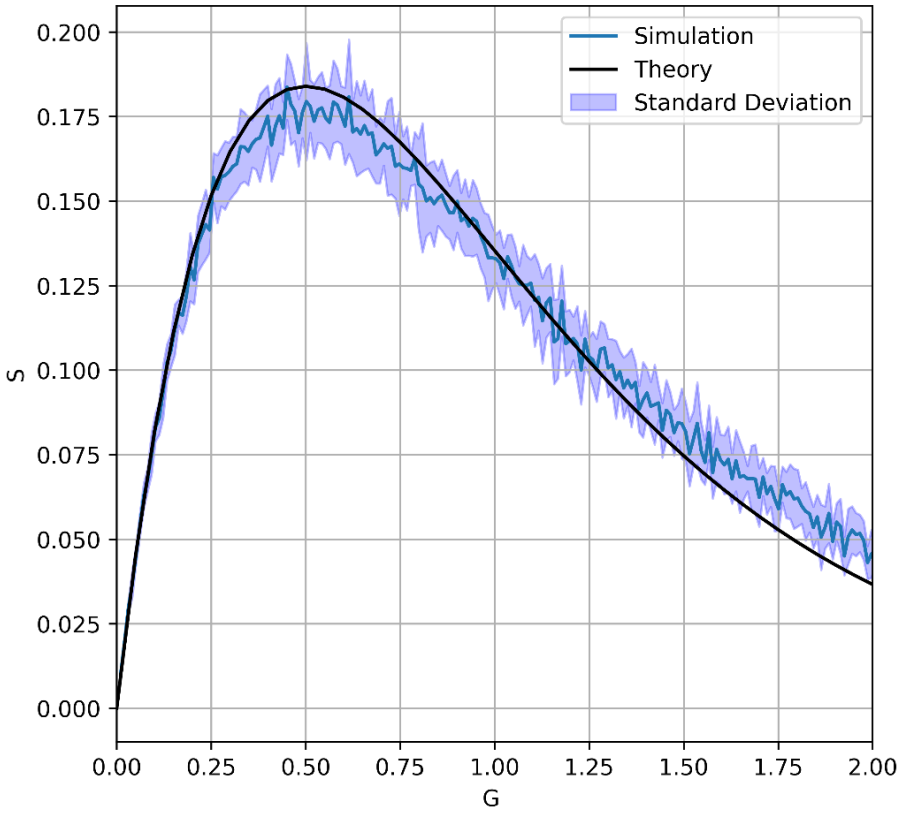

Figure 4.4: Throughput comparison between theory and ns-3 simulations

4.3. Evaluation Scenarios

In this section we present the main aim of this work, to compute the throughput of a LoRa/LoRaWAN network. Our approach is to analyse the results from theoretical models and simulations and make a comparison of the results obtained. We begin by investigating two different scenarios based on the distribution of the EDs and the assignment of the SFs. The scenarios are as follows:

- Scenario 1 - EDs are assigned based on the area which is allotted to a particular SF based on its contribution to the total possible capacity provided by the network.

- Scenario 2 - EDs are assigned based on the sensitivity of a SF and the range covered by a SF**.**

We define and compute the parameters required to formulate the above mentioned scenarios. We use Friis free space equation [35] to compute the radius (R) and obtain different values for R as we vary path loss.

$$\frac{P_r}{P_t} = G_t * G_r * (\frac{c}{4\pi f})^2 * (\frac{1}{\mathrm{R}})^{\alpha} \quad (4.8)$$

where,

- P_r is the received power, in mW
- P_t is the transmitted power, in mW
- G_t is the transmitter gain
- G_r is the receiver gain
- c is the speed of light in vacuum, in m/s
- f is the frequency, in Hz
- R is the distance from the transmitter, in m
- α is the path loss exponent

We consider the gain of the transmitter and the receiver (G_t, G_r) to be *1*. We re-arrange Equation 4.8 to serve our purpose and we obtain Equation 4.9.

$$\mathrm{R} = \left(\frac{P_t}{P_r} * \left(\frac{c}{4\pi f}\right)^2\right)^{1/\alpha} \quad (4.9)$$

We consider the value for $f = 868\,MHz$, the frequency LoRa operates in Europe as stated in Table 1.1. $P_r = 2 * 10^{-14} mW$, it is the sensitivity corresponding to SF 12 as stated in Table 2.3. We consider this value for P_r so that every ED reaches the GW. $P_t = 25\,mW$ for the maximum output power of the *ED*s, taken from [18]. We substitute these values in Equation 4.9 to compute the radius of our test setup. Figure 4.8 shows the changes in R as we vary α.

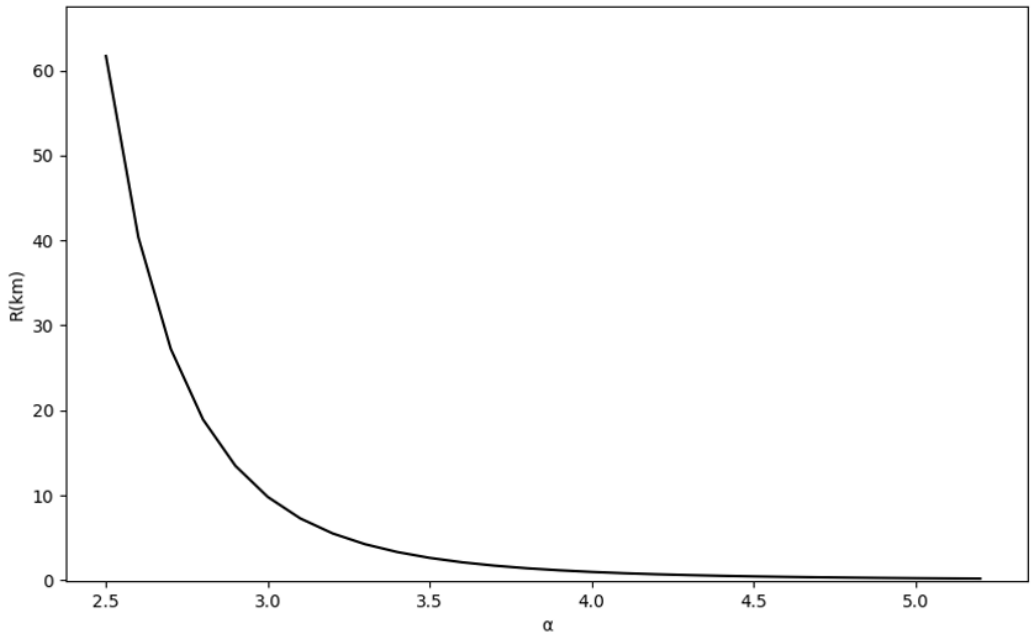

Figure 4.8: Change in Radius (R) with different values of α

We discussed in Section 4.2.2 that LoRaWAN follows the ALOHA protocol and the maximum value for throughput (S_{max}) is obtained at $G_{max} = 0.5$. We now investigate how the network would behave under optimal conditions considering $G = G_{max}$. We compute the number of end devices that will be assigned a particular SF at G_{max}. We also obtain the total number of EDs the network can handle by taking the sum of EDs for each SF. This illustrates the optimal number of EDs the network can handle. We use this information when testing our scenarios i.e., Scenario 1 and Scenario 2. To compute the end devices assigned to a SF, we use Equation 4.10.

$$N_{SF} = G * \frac{R_{SF}}{\lambda * L_P} \quad (4.10)$$

where,

- N_{SF} gives the end devices using a particular SF
- R_{SF} is the bit rate of a SF
- λ is the packet rate
- L_P is the size of the packet

We set $\lambda = 1/100$, $L_P = 10\ bytes$ and R_{SF} corresponds to the selected SF from Table 2.1. We obtain the total number of EDs in the network to be 7515 under optimal conditions.

We obtain values for various parameters which we use for our experimental setup in this work. Table 4.1 summarises the parameters and their values considered for the evaluation purposes.

Table 4.1: System parameters

Parameters	Value
End devices	7515
Network Radius	9.8 km
Transmission Power	25 mW
Spreading Factor	7-12
Carrier frequency	868 MHz
Bandwidth	125 kHz
Path loss exponent	3-4

4.3.1. Scenario 1

In this scenario, we distribute the area between the SFs based on their contribution to the total capacity of the network. We use the values of the parameters from Table 4.1 to design our experimental setup. Table 4.2 illustrates the bit rates and the contribution percentage of each SF to the total capacity.

Table 4.2: SF contribution to total capacity

SF	***R_b (bps)***	***Total Capacity(bps)***	***% R_b***
7	5470	12025	45.5%
8	3125		26%
9	1760		14.6%
10	980		8.15%
11	440		3.65%
12	250		2.1%

We try to find the condition for which the network can perform at its optimal capacity, thus allowing the end devices to transmit at full capacity and reduce the probability of lost packets. From Table 4.2, it is clear that the contribution of *SF7* amounts to almost half of the total capacity of the network, so we assign *SF7* with the percentage of the area equivalent to its contribution, the area distribution is illustrated in Figure 4.10. This allows us to assign more devices to the lower *SFs*, the larger the *SF*, less devices assigned to it.

We compute the radius (R) of our setup using Equation 4.9 for α = 3. Then the radius for each SF is computed as R is divided into multiple rings. The radii of the annuli's can be computed with Equation 4.11, and then the EDs are assigned to each annulus based on Equation 4.12.

$$R_k = \sqrt{\%R_k * {A}/{\pi}} - \sum_{i=1}^{k-1} R_i \tag{4.11}$$

where,

- $\%R_k$ is the percentage of capacity contributed by a spreading factor
- A is the total simulation area
- R_i is the radius of the previous annulus

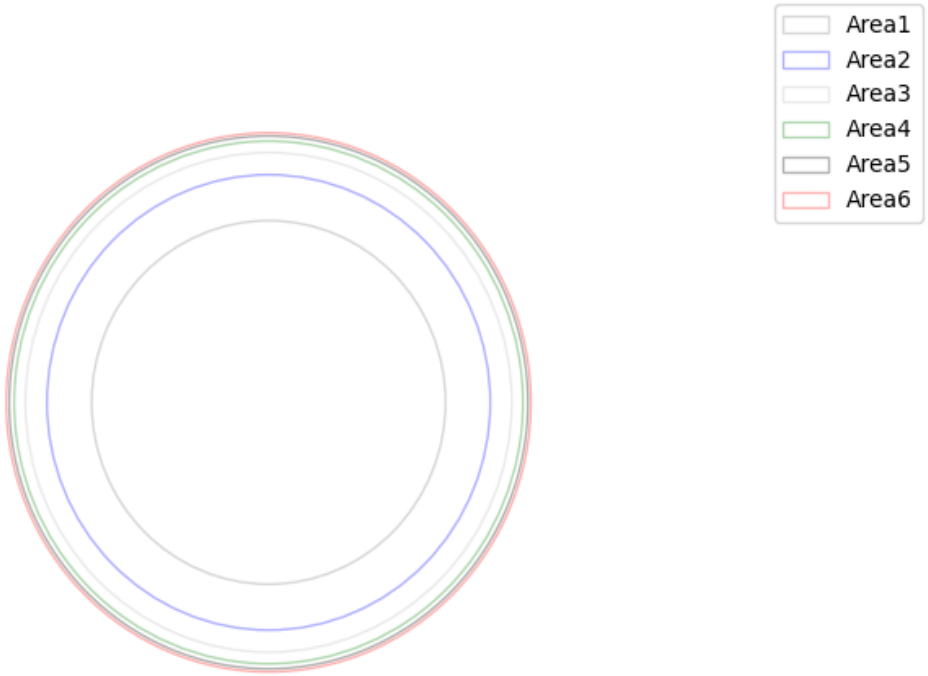

Figure 4.10: Area distribution for the proposed scenario

$$N_k = N * {}^{A_k}/_{A} \tag{4.12}$$

where,

- N_k is the number of EDs in an annulus
- N is the total number of end devices in the network
- A_k is the area of an annulus
- A is the total area of the simulation area

The distribution of the end devices in the network can be seen in Figure 4.11. This scenario is optimal in terms of the assignment of EDs to a SF as it aims to maximize the capacity of the network, thus assigning more devices to the SF providing higher capacity. However, this strategy has a drawback and might not be the best practice in certain conditions, when the ED is too far away and the sensitivity is too low to communicate with the GW. In that case even if the EDs are assigned to certain SF, the packets are lost and moreover the channel remains busy thus affecting the overall network performance.

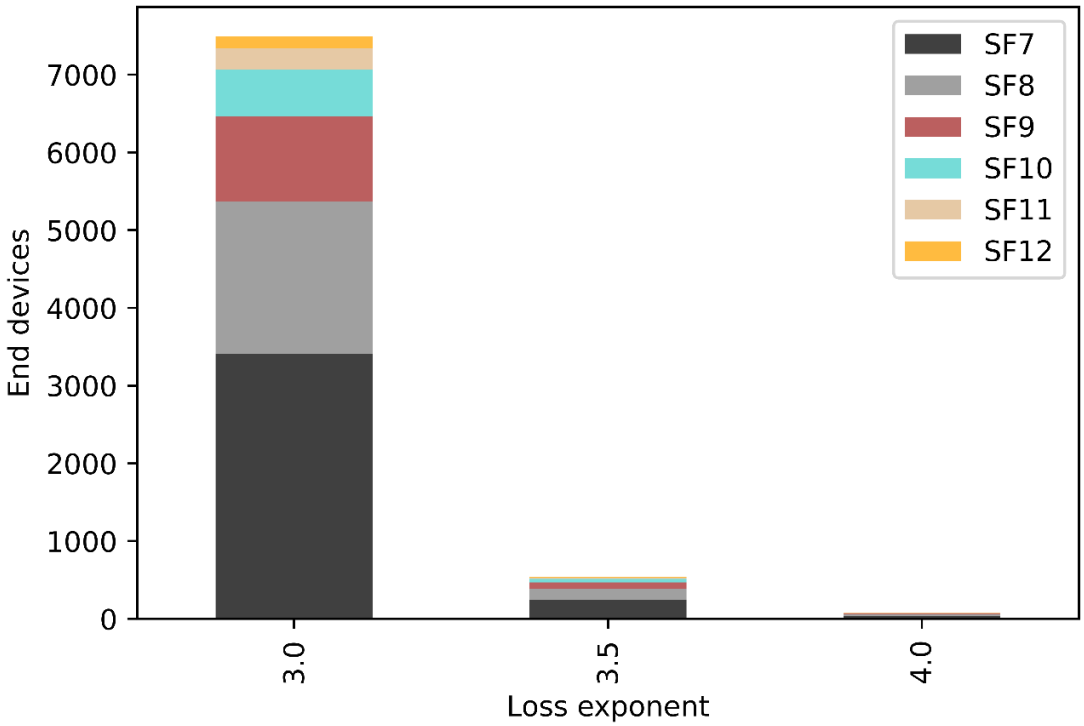

Figure 4.11: Distribution of EDs in the network

The total throughput provided by the network and the individual contributions of SFs can be seen in Figure 4.12. We see the lower SFs contributing more than the higher SFs to the capacity courtesy to more area and thus higher number of EDs assigned to them. However as the propagation gets worse, this approach is not the most suitable as it continues to allocate higher number of devices to the lower SFs, whereas use of higher SFs might be more beneficial owing to their robustness.

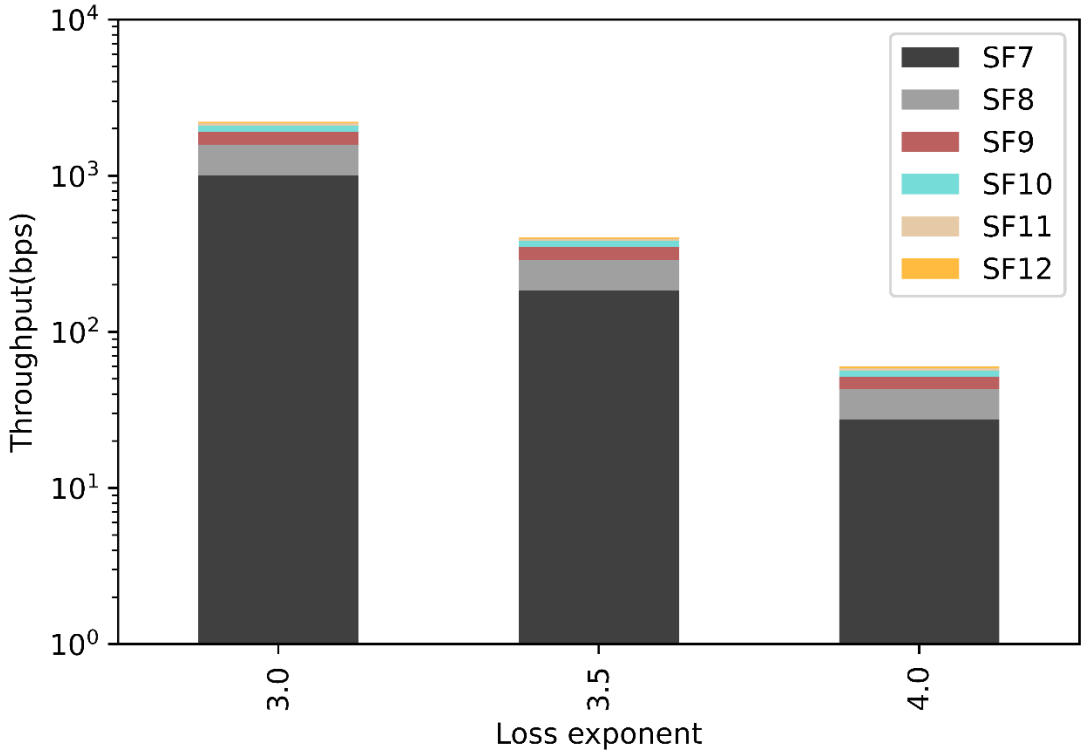

Figure 4.12: Throughput contribution of spreading factors

4.3.2. Scenario 2

In this scenario, we compute the maximum range a SF can cover taking the sensitivity into account. The maximum range or radius is computed using Equation 4.9 and the lowest value of sensitivity among all the SFs in order to make sure that all the EDs can reach the GW. We then calculate the range for each individual SF and keeping the density of the EDs same as in the previous scenario, the EDs are assigned a SF.

As an example of this procedure, suppose α = 4 and we consider the value for SF12 from Table 2.3, which gives us the value for R = 0.986 km using Equation 4.9. Table 4.3 gives the values for the distance threshold for different values of α of all the SFs using the above mentioned settings.

Table 4.3: Distance threshold (l_m) for SFs

SF	l_m (km)		
	$\alpha = 3$	$\alpha = 3.5$	$\alpha = 4$
7	0-3.616	0-1.122	0-0.466
8	3.616-4.556	1.122-1.367	0.466-0.554
9	4.556-5.74	1.367-1.667	0.554-0.659
10	5.74-7.232	1.667-2.032	0.659-0.784
11	7.232-8.427	2.032-2.317	0.784-0.879
12	8.427-9.815	2.317-2.64	0.879-0.986

The distribution of the EDs can be seen in Figure 4.13 with most devices being assigned to higher SFs which is not optimal as the full capacity of the network is not achieved. *SF7* provides the largest bit rate, while *SF12* has the least. As *SF12* is assigned larger portion of EDs, the network underachieves as those devices transmit with the lowest available data rate.

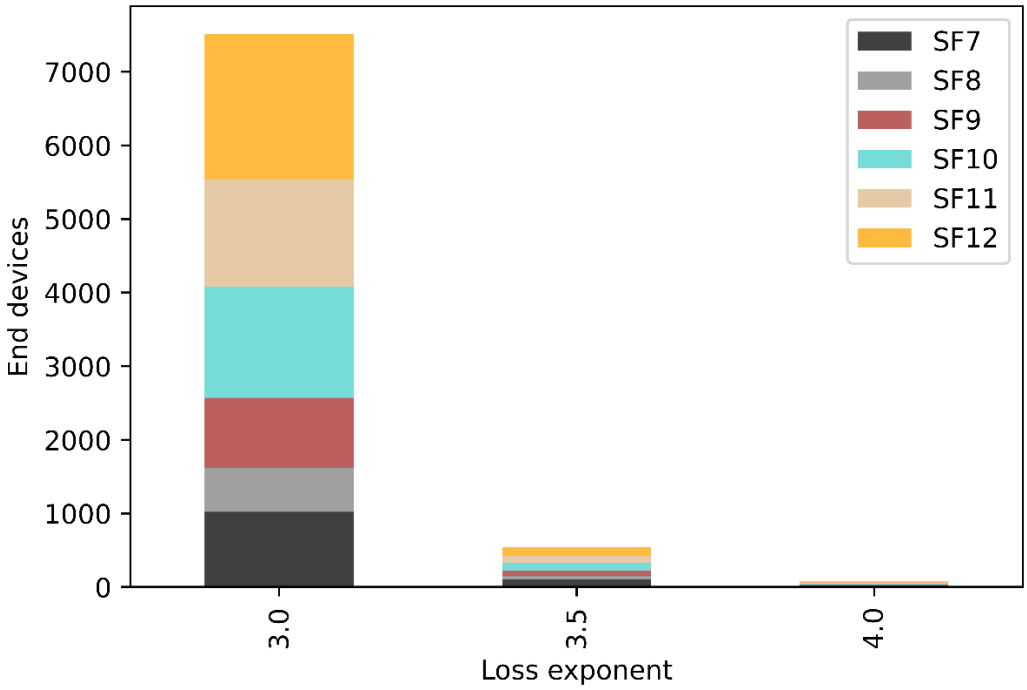

Figure 4.13: Distribution of end devices in the network

The throughput provided by the network and the contribution by each SF can be seen in Figure 4.14. We see even though more EDs are assigned higher SFs, their contribution to the total throughput is very low compared to the lower SFs.

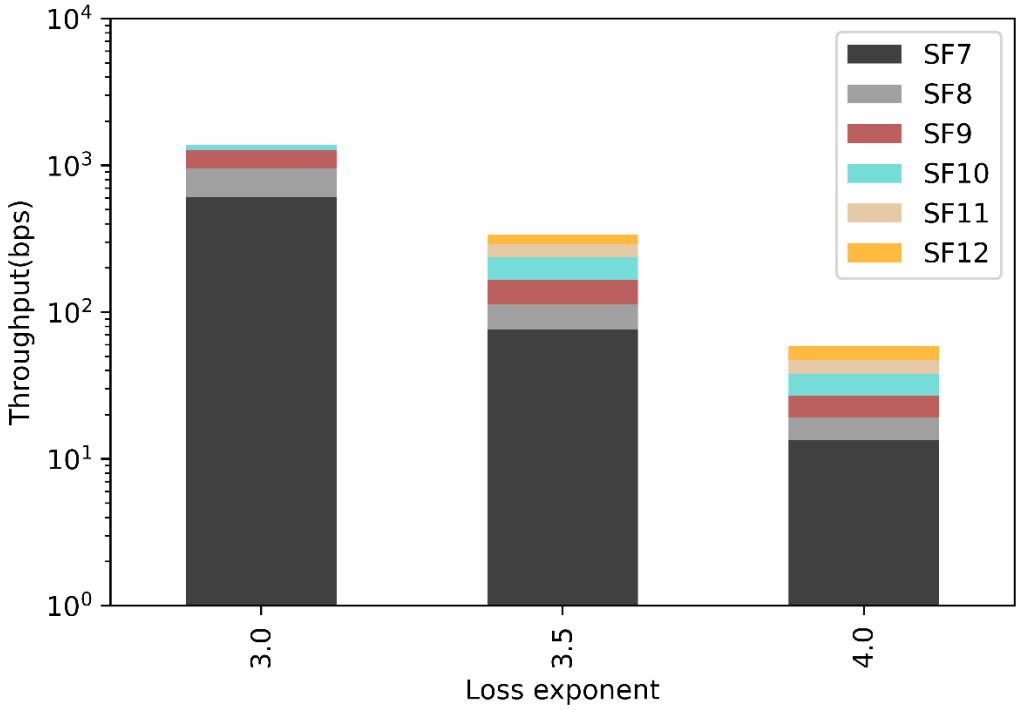

Figure 4.14: Throughput contribution of spreading factors

4.3.3. Simulation results

After the analysis of the theoretical models, we simulate the network using ns-3. We simulate the network with two sets of configuration, with and without implementing propagation losses due to shadowing.

4.3.3.1. Results with no shadowing

We run the simulations in ns-3 with the same parameters as Scenario 2, we observe the distribution of EDs and compute the throughput provided by the network. Figure 4.15 shows the distribution of EDs in the network as we vary the path loss. We notice that for α = 3 all the EDs are assigned either SF7 or SF8, but as the propagation conditions get worse, the proportion of EDs assigned the higher SFs increases as well. The reason for such behaviour is the low sensitivity requirements for higher SFs.

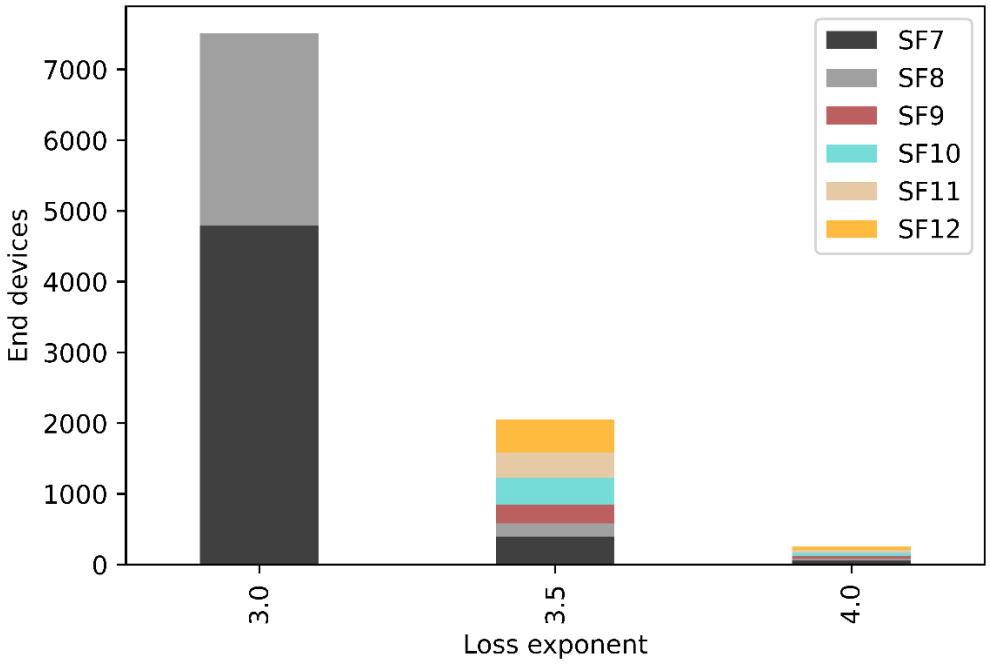

Figure 4.15: Distribution of EDs in the network without shadowing

The capacity of the network computed from the simulations and individual contributions of each SF is illustrated in Figure 4.16. Again there is a downward trend in the total throughput achieved as the propagation conditions degrade. We see the SF7 providing most of the capacity for α = 3.

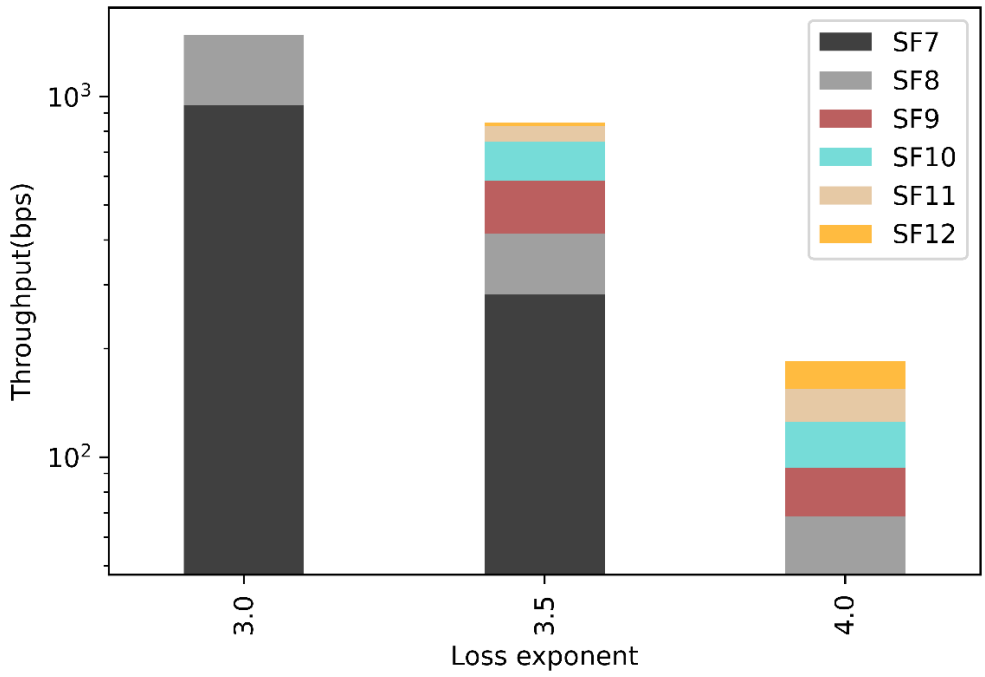

Figure 4.16: Throughput contribution of spreading factors

4.3.3.2. Results with shadowing

In order to further analyse the network, we investigated its behaviour in a realistic propagation scenario. In addition to propagation losses already accounted for, we take into account the losses due to the buildings and the impact of shadowing. The LoRaWAN module [22] has a loss model that implements the shadowing losses caused by buildings. The design of the structures is inspired by the layout of Manhattan area and the measurements and values are used to replicate that area. In case the position of the ED and the building coincide, the ED is assumed to be inside the building. Figure 4.17 shows the distribution of the EDs in this scenario.

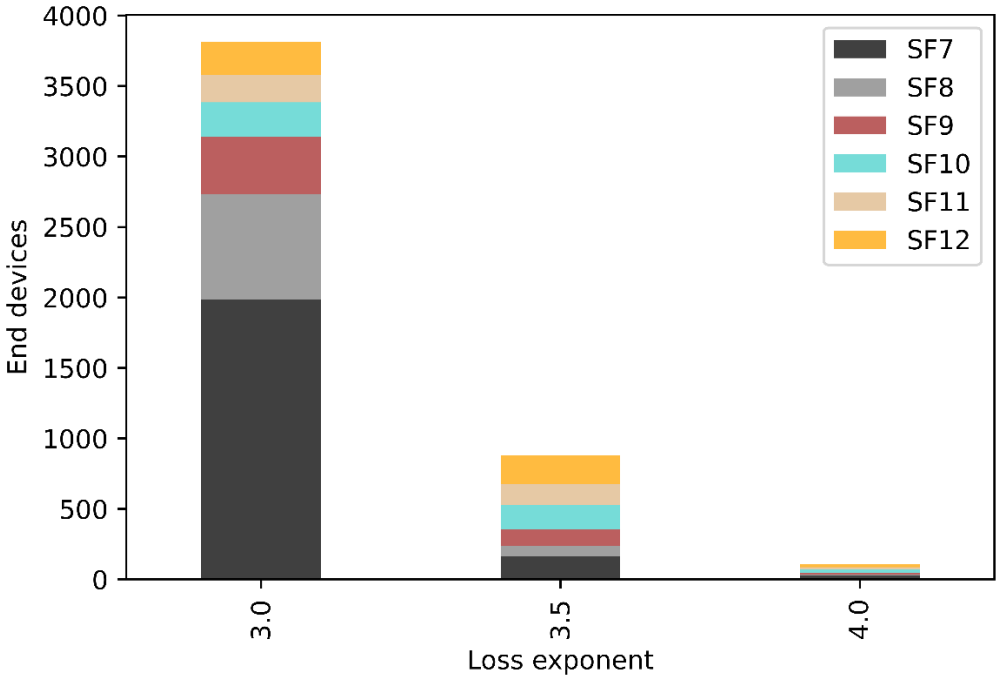

Figure 4.17: Distribution of EDs in the network with shadowing

Figure 4.18 depicts the change in the throughput of the network as we vary the path loss exponent. As expected, the contribution of the lower SFs reduce as the propagation conditions get worse and we also see the total capacity offered by the network reduce.

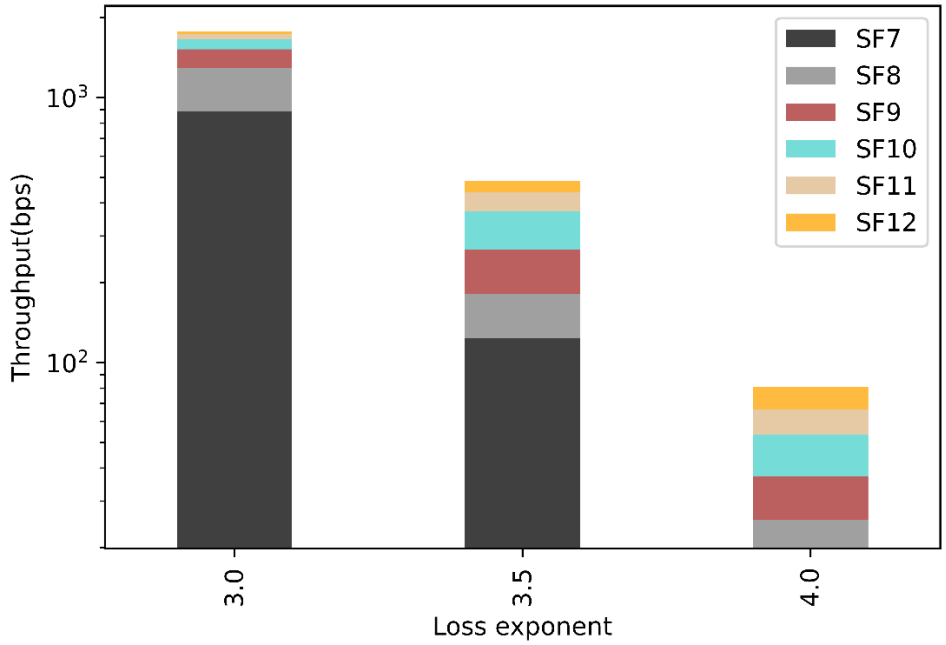

Figure 4.18: Throughput of the network with shadowing

4.4. Results and discussion

As the purpose of this work is to understand and determine the actual capacity of a LoRaWAN network, we will be discussing the results obtained for throughput for Scenario 2 and the simulation results.

We see that for α = 3 in Figure 4.14 and Figure 4.16, the throughput in both the cases does differ much. However, in Figure 4.16, the contribution only comes from SF7 and SF8 because all of the devices being assigned these two SFs contrary to what we expect from a theoretical model as seen in Scenario 2. The possible reason for this is that due to no heavy losses and attenuation, the GW is able to receive the packets from SFs with higher sensitivity values. The difference is more considerable as we increase the value of α, with simulation results performing better than the theoretical approach of Scenario 2. This is due to the fact that in theoretical models we expect all the packets colliding to be destroyed, but that is not that case due to 'capture effect'- an important feature in LoRaWAN. Due to this feature the packet with higher power out of the two colliding packets is still received. We observe the downward trend in both the cases but the results from simulation demonstrate better performance, thus providing higher capacity.

In the next simulation when we consider the shadowing caused by the buildings, we notice in Figure 4.17 that for α = 3 EDs are assigned higher SFs as well. This behaviour can be explained even if an ED with lower SF is close to the GW but due to the shadowing effect cannot be received due to the strict restrictions on

the sensitivity. In this scenario higher SFs prevail due to their low sensitivity demands. As the conditions worsen the capacity provided by the network decreases as well as the difference in the performance become more noticeable.

We summarise the simulation results from the two sets of configurations. We compare the behaviour based on the difference in assigned EDs and throughput. Figure 4.19 illustrates the difference in the number of EDs that are assigned a SF. The network without shadowing performs better by having almost twice the number of EDs. This behaviour can be explained due to the additional losses in the network due to shadowing.

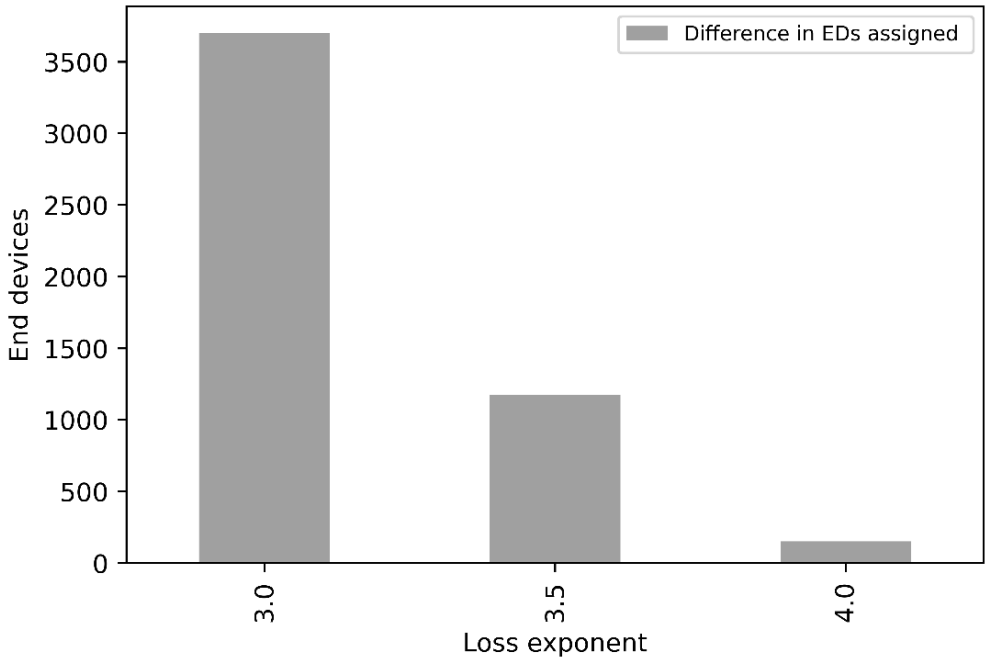

Figure 4.19: Difference in assigned EDs with and without shadowing

We compare the throughput achieved in both configurations to analyse the performance of the network. In Figure 4.20, we present the difference in total throughput of both the cases (i.e., with and without shadowing). We take results from no shadowing as baseline and compare the results from both configurations. For α = 3, throughput for the network with shadowing exceeds the throughput without shadowing. This is due to the reason that majority of EDs are assigned SF7 as seen in Figure 4.15. This results in too much load for SF7 and the interference among the same SF packets. For this reason the packets are lost and do not add to the total throughput of the network. On the contrary in the case of network with shadowing, the EDs are distributed among different SFs as seen in Figure 4.17. As α increases, network without shadowing performs better due to distribution of EDs not restricted to only few SFs.

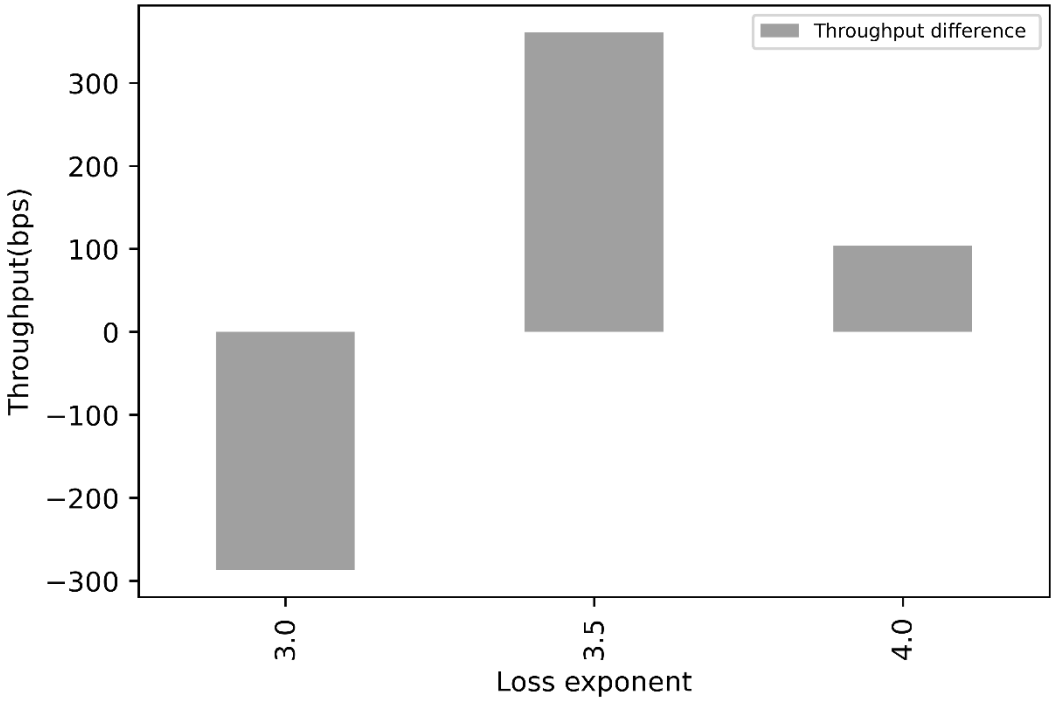

Figure 4.20: Throughput comparison of with and without shadowing

In Table 4.4, we summarise theoretical model and simulation results, with total throughput rounded off to the nearest integer.

Table 4.4: Summary of theoretical and simulation results

Parameters		Scenario 2 (Theoretical)	Simulation (No shadowing)	Simulation (Shadowing)
End devices		7515	7515	3813
Total Throughput (bps)	$\alpha = 3$	1387	1484	1771
	$\alpha = 3.5$	337	845	484
	$\alpha = 4$	59	185	81

Chapter 5: Conclusions and Future work

The aim of this work is to study the performance and scalability of LoRa/LoRaWAN networks. After a brief introduction to IoT paradigm and technologies, we have introduced LoRa/LoRaWAN in depth. We have also reviewed some of the past research and followed that with the evaluation of LoRaWAN network.

It is important to know how the network will behave under different conditions and gauge its performance so that it suits the needs before it is deployed in real world conditions. In this work, we have presented theoretical models and computed the network throughput. In the first model, we have distributed the area based on the contribution of a SF to the network capacity and then assigned the EDs. In the second model, we have assigned the EDs based on the distance threshold of SFs. The network is studied with 7515 EDs and a radius of 9.8 km, the values obtained for a network under optimal conditions. We have simulated the network using ns-3 with the same parameters and computed the network throughput. We perform the simulations with the GW located at the centre of the circle under two different configurations - with and without shadowing. Finally, we compare the results of theoretical model with the simulation results for the assignment of SF to EDs and network throughput.

On comparing the results, we notice that as the propagation conditions get worse the network suffers and the throughput provided by the network reduces. This behaviour is due to the increase in the propagation losses which affect the channel and result in higher number of lost packets. The results from simulations fare better than the theoretical results. Throughput obtained from simulations is higher than theoretical model even with bad propagation conditions. This is due to the fact that not all colliding packets are lost because of capture effect property of LoRa/LoRaWAN and thus contribute to the total network throughput. On comparing the results from two sets of simulation configurations, we conclude that more EDs are assigned in the network with no shadowing. However contrary to expectations, for path loss exponent = 3, throughput achieved in network with shadowing is higher.

A single LoRa/LoRaWAN network is intended to connect thousands of devices to the internet. For the sustainability of this technology it important for these devices to be cheap from economic point of view. On one hand, the mass production of these devices, even though cheap, add considerably to the economy of the hardware development industry. On the other hand, manufacturing these devices can have negative environmental impact due to harmful emissions.

The end devices spread across a LoRa/LoRaWAN network operate on batteries with very small power consumption. The sporadic use of battery enables it to last for years, thus making it highly energy efficient.

The impact of this work on economy, privacy and human rights is also considered. This work adheres to the privacy policy of LoRa/LoRaWAN technology. LoRa/LoRaWAN includes several security protocols including data integrity and confidentiality protection. It implements end-to-end encryption for data exchanged between the end devices and the servers. Hence, the use of this technology should not be considered a threat in security aspect.

This work opens up possibilities of future studies. An example could be to evaluate the performance of the network under similar conditions and increasing the number of gateways. The gateways could be located at the periphery of the radius, in order to determine the impact on the total capacity of the network. Another study could be carried out which would allow us to simulate the optimal scenario (Scenario 1) using ns-3, so that we evaluate the performance under those conditions. We expect in this scenario as the EDs will be optimally distributed, the network throughput will be higher. By adding more gateways, we expect the performance of the network will be further enhanced in this scenario.

This GitHub repository contains all the code used in this work.

Acronyms

3GPP 3rd Generation Partnership Project

ABP Activation By Personalization

ACK Acknowledgement

ADR Adaptive Data Rate

AS Application Server

BLE Bluetooth Low Energy

BW Bandwidth

CCTV Closed-Circuit Television

CR Coding Rate

CRC Cyclic Redundancy Check

CSMA Carrier-Sense Multiple Access

CSS Chirp Spread Spectrum

DSSS Direct Sequence Spread Spectrum

ED End Devices

eDRX Extended Discontinuous Reception

ETSI European Telecommunications Standard Institute

FDD Frequency Division Duplex

FDMA Frequency Division Multiple Access

FEC Forward Error Correction

GW Gateway

IoT Internet of Things

ISM Industrial, Scientific, and Medical

LoS Line of Sight

LPWAN Low Power Wide Area Network

LR-WPAN Low Rate Wireless Personal Area Networks

LTE Long Term Evolution

LTE-M Long Term Evolution for Machines

MAC Medium Access Protocol

NB Narrowband

NF Noise Figure

NS Network Server

OTAA Over-The-Air Activation

P-ALOHA Pure ALOHA

PDR Packet Delivery Ratio

PER Packet Error Ratio

PHY Physical Layer

PSM Power Saving Mode

QoS Quality of Service

RPMA Random Phase Multiple Access

S-ALOHA Slotted ALOHA

SF Spreading Factor

SNR Signal to Noise Ratio

SUN Smart Utility Networks

TDMA Time Division Multiple Access

ToA Time on Air

TVWS TV white space

UHF Ultra-High Frequency

UNB Ultra Narrowband

VoLTE Voice over Long-Term Evolution

Wi-SUN Wireless Smart Utility Networks

References

[1] Farrell, S., Ed., "Low-Power Wide Area Network (LPWAN) Overview", RFC 8376, DOI 10.17487/RFC8376, May 2018, https://www.rfc-editor.org/info/rfc8376

[2] Network overview of Sigfox. Retrieved from https://build.sigfox.com/sigfox

[3] AN1200.22 - LORA Modulation Basics. Retrieved from https://www.semtech.com

[4] LoRa Alliance. “RP002-1.0.1 LoRaWAN Regional Parameters”, 2020

[5] LoRa SX1301 Datasheet (2017, June). Retrieved from https://www.mouser.com/datasheet/sx1301

[6] SX1272/73 860 MHz to 1020 MHz Low Power Long Range Transceiver (March, 2017). Retrieved from https://www.mouser.com/datasheet/sx1272

[7] What is LoRaWAN Specification. Retrieved from https://lora-alliance.org/about-lorawan

[8] LoRaWAN 1.1 Specification: https://lora-alliance.org/specification_v1.1.pdf

[9] I. Howitt and J. A. Gutierrez, "IEEE 802.15.4 low rate - wireless personal area network coexistence issues". *IEEE Wireless Communications and Networking*, vol.3, pp. 1481-1486, 2003

[10] F. Van den Abeele, J. Haxhibeqiri, I. Moerman, J. Hoebeke. “Scalability analysis of large-scale LoRaWAN networks in ns-3”. *IEEE Internet of Things Journal*, vol.4, pp. 2186 - 2198, 2017

[11] Reynders, B., Wang, Q., Pollin, S. “A LoRaWAN module for ns-3: implementation and evaluation”. *WNS3 '18: Proceedings of the 10th Workshop on ns-3*. 61-68. 10.1145/3199902.3199913, 2018

[12] Zorbas, D., Abdelfadeel, K., Kotzanikolaou, P., Pesch, D. “TS-LoRa: Time-slotted LoRaWAN for the Industrial Internet of Things”, *Computer Communications*, Volume 153, pp. 1-10, 2020.

[13] A. Hoeller, R. D. Souza, H. Alves, O. L. Alcaraz López, S. Montejo-Sánchez and M. E. Pellenz, "Optimum LoRaWAN Configuration Under Wi-SUN Interference," in *IEEE Access*, vol. 7, pp. 170936-170948, 2019.

[14] L. Beltramelli, A. Mahmood, P. Österberg and M. Gidlund, "LoRa Beyond ALOHA: An Investigation of Alternative Random Access Protocols," in IEEE Transactions on Industrial Informatics, vol. 17, no. 5, pp. 3544-3554, 2021.

[15] Lavric, A., Popa, V. “Performance Evaluation of LoRaWAN Communication Scalability in Large-Scale Wireless Sensor Networks”, *Hindawi*, Volume 2018

[16] Rajab, H., Cinkler, T., Bouguera, T. “IoT scheduling for higher throughput and lower transmission power.” *Wireless Networks*, 27, 2021.

[17] L. A. Hassnawi, R.B Ahmad, A. Yahya, M. Elshaikh, A. Al-Rawi, Z. G. Ali. “Performance Analysis of Motorway Surveillance System Based on Wireless Ad Hoc Camera Network (WAHCN)”. *Journal of Communications and Information Sciences*, 2, 59, 2012.

[18] ETSI TR 103 526 V1.1.1 (2018): Technical characteristics for Low Power Wide Area Networks Chirp Spread Spectrum (LPWAN-CSS) operating in the UHF spectrum below 1 GHz: https://www.etsi.org/deliver/etsi_tr.pdf

[19] ETSI TR EN 300 220-1 V2.4.1 (2012): Electromagnetic compatibility and Radio spectrum Matters (ERM); Short Range Devices (SRD); Radio equipment to be used in the 25 MHz to 1000 MHz frequency range with power levels ranging up to 500 mW: https://www.etsi.org/deliver/etsi_en/300200_300299/.pdf

[20] LoRaWAN Duty Cycle. Retrieved from https://www.thethingsnetwork

[21] ns-3 network simulator: https://www.nsnam.org/

[22] LoRaWAN ns-3 module: https://github.com/signetlabdei/lorawan

[23] Gokhale, P., Bhat, O. and Bhat, S. "Introduction to IOT." *International Advanced Research Journal in Science, Engineering and Technology* 5, no. 1, pp. 41-44, 2018.

[24] Krčo, S., Pokrić, B. and Carrez, F. "Designing IoT architecture(s): A European perspective," *2014 IEEE World Forum on Internet of Things (WF-IoT)*, pp. 79-84, 2014

[25] Ergen, S.C. "ZigBee/IEEE 802.15. 4 Summary." *UC Berkeley, September* 10, no. 17, pp. 11, 2004

[26] Gomez, C. and Paradells, J. "Wireless home automation networks: A survey of architectures and technologies." *IEEE Communications Magazine* 48, no. 6, pp. 92-101, 2010.

[27] Gomez, C., Oller, J. and Paradells, J. "Overview and evaluation of bluetooth low energy: An emerging low-power wireless technology." *Sensors* 12, no. 9, pp. 11734-11753, 2012.

[28] Sigfox: Retrieved from https://www.sigfox.com/en

[29] Mekki, K., Bajic, E., Chaxel, F. and Meyer, F. “Overview of cellular LPWAN technologies for IoT deployment: Sigfox, LoRaWAN, and NB-IoT.” In *2018 ieee international conference on pervasive computing and communications workshops (percom workshops)*, pp. 197-202. IEEE, 2018.

[30] Weightless SIG: https://www.weightless.org/

[31] Weightless Alliance: https://www.weightless-alliance.org/

[32] Liao, C.H., Zhu, G., Kuwabara, D., Suzuki, M. and Morikawa, H. “Multi-hop LoRa networks enabled by concurrent transmission.” *IEEE Access*, *5*, pp.21430-21446, 2017.

[33] Augustin, A. et al. “A Study of LoRa: Long Range & Low Power Networks for the Internet of Things.” *Sensors*, 16, 9, p.1466, 2016.

[34] LoRa: https://www.semtech.com/lora

[35] Ramesh, R., Arunachalam, M., Atluri, HK., Kumar, SC., Anand, S.V.R., Arumugam, P., Amrutur, B. “LoRaWAN for smart cities: experimental study in a campus deployment”, *LPWAN Technologies for IoT and M2M Applications,* Academic Press, 2020, Pages 327-345.